Supplementary Information

Supplementary Figures. Figures S1–S6.

Supplementary Tables

Table S1. Clinical information of the NB specimen used for single cell RNA-Seq, related to Figure 1.

Table S2. Basic information for single-cell datasets of eight tumor samples, related to Figure 1.

Table S3. The table shows differentially expressed genes of identified 6 cell clusters/states in NB cells, related to Figure 2.

Table S4. Enriched upregulated pathways in the cells of Cluster 3 versus other malignant cells, related to Figure 4.

Table S5. The 'starter'-cell signature for Cluster 3. Top 150 genes identified by Seurat function FindAllMarkers, related to Figure 4.

Table S6. Reagents, accession numbers and software.

Supplementary Figures

Figure S1(1 of 5). Related to Figure 1.

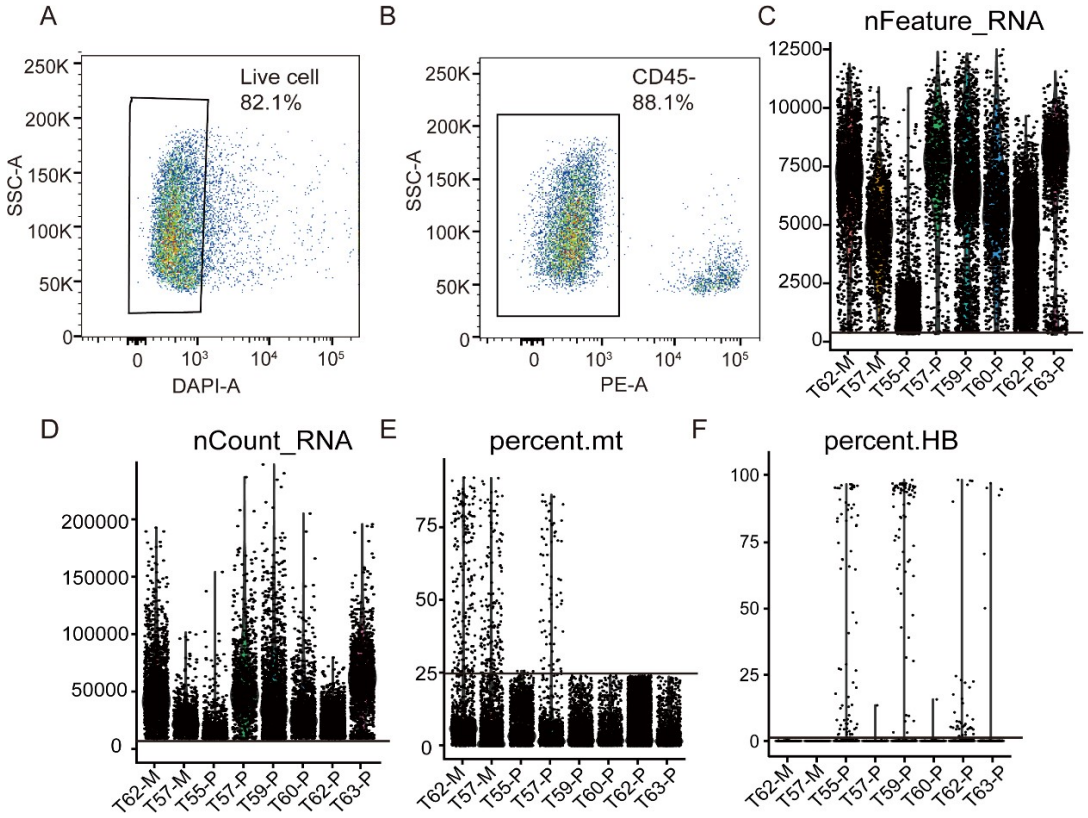

Figure S1(2 of 5). Related to Figure 1.

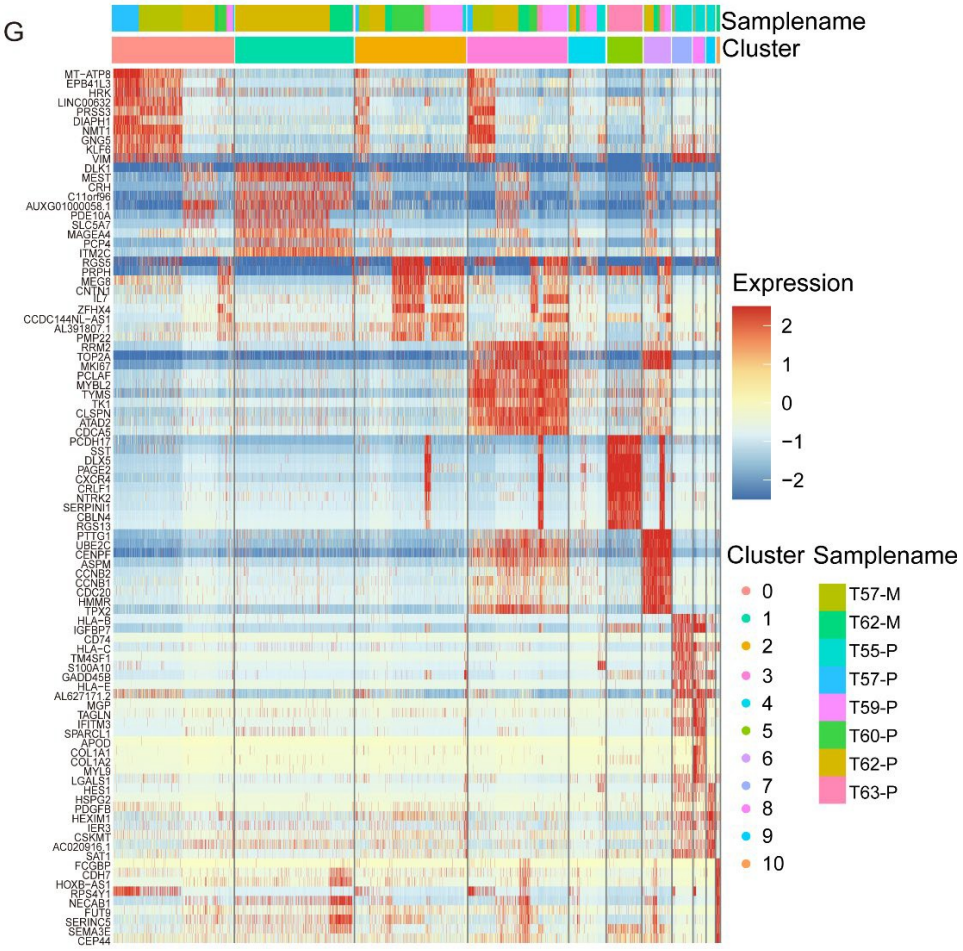

Figure S1(3 of 5). Related to Figure 1.

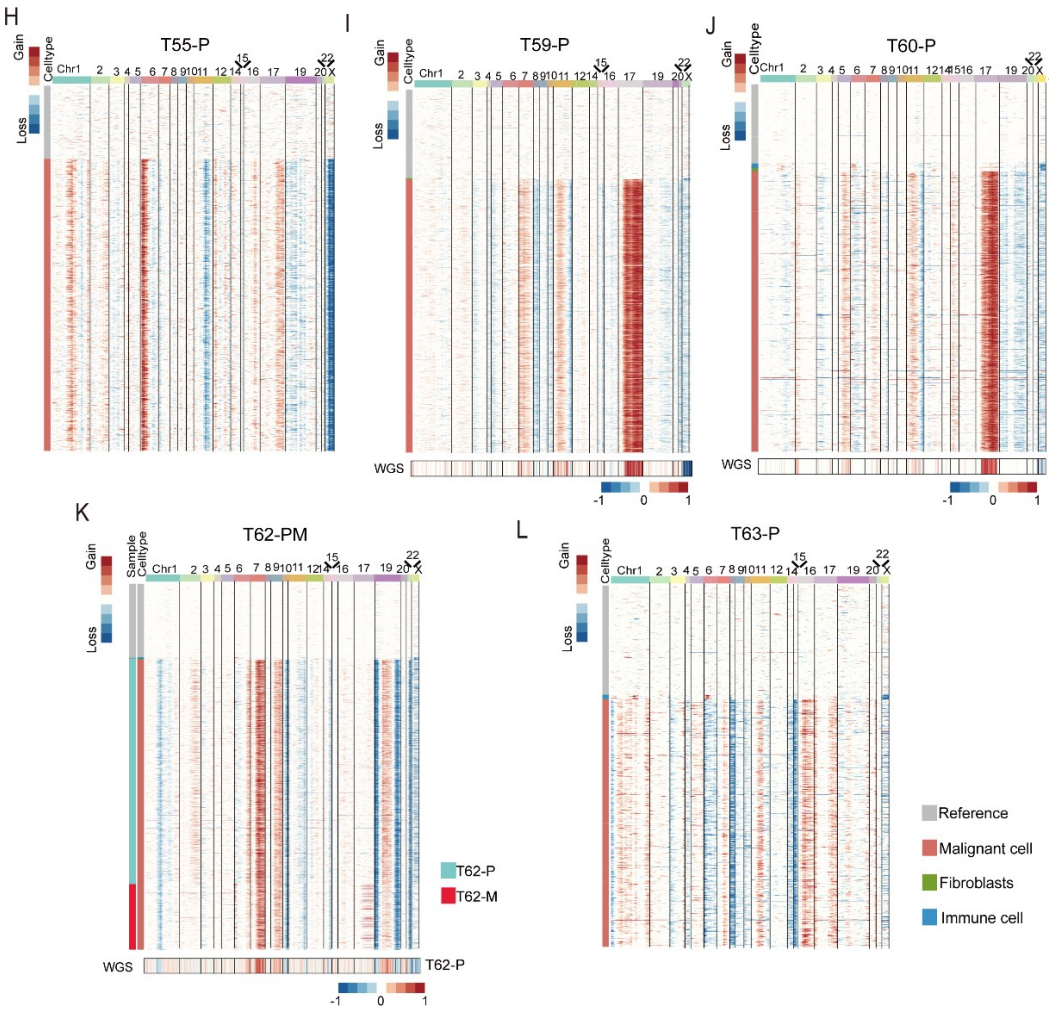

Figure S1(4 of 5). Related to Figure 1.

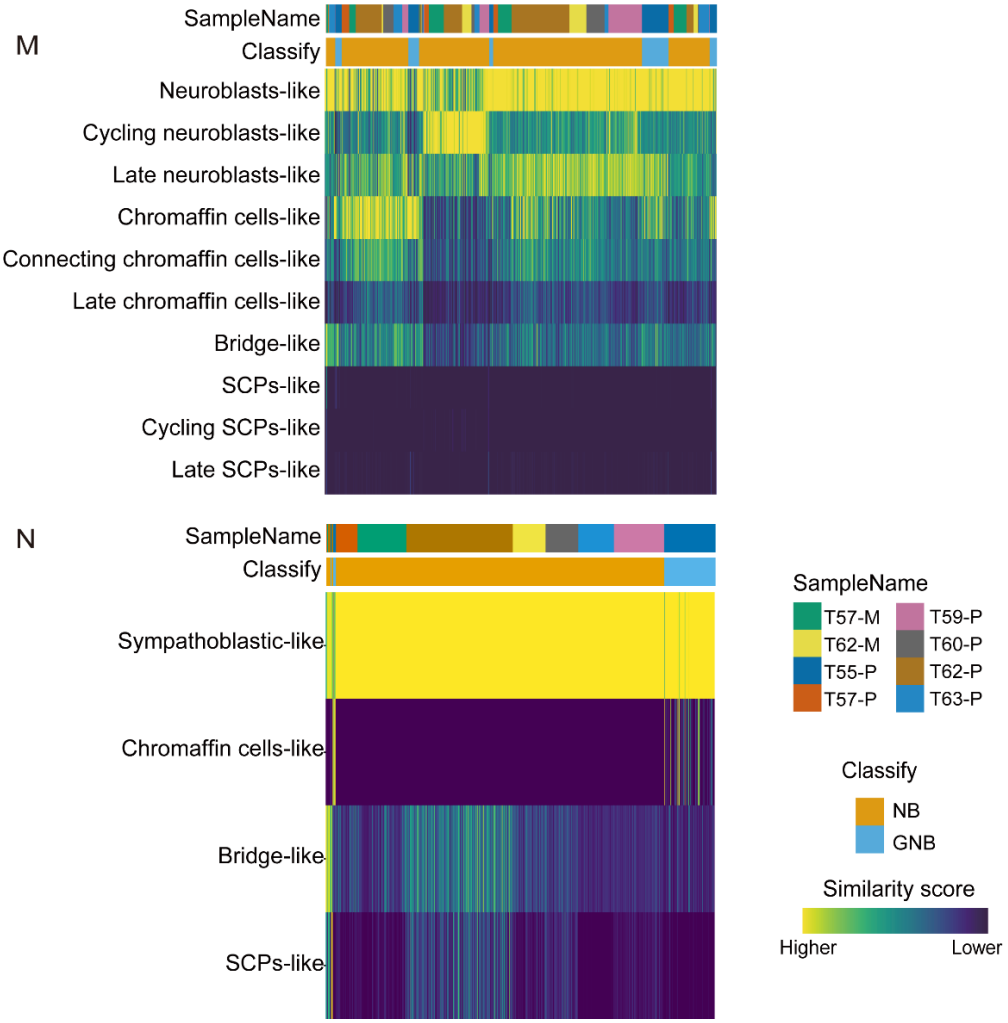

Figure S1(5 of 5). Related to Figure 1.

A-B. Fluorescence-activated cell sorting (FACS) was performed on dissociated tumor samples to isolate the cells in the inflammatory infiltrate and DAPI-positive dead single cells. Representative figure showing the gating strategy after staining cells with CD45 (inflammatory infiltrate cells) and DAPI (dead cells).

C-F. Histograms showing the distribution of total nFeature (**C**), nCount (**D**), mitochondrial reads per cell (**E**) and hemoglobin reads per cell (**F**). The histograms are color coded according to the original patient identity. The black dashed lines indicate the cutoffs used for selecting high-quality cells.

G. Heatmap showing the top ten differentially expressed genes in each cluster based on the UMAP plots shown in Figure 1C.

H-L. Inferred copy number profiles of neuroblastoma cells using InferCNV with normal sympathoblasts as reference. Below: Copy number profiles of the same tumors derived from whole genome sequencing data (WGS).

M-N. Heatmaps with the similarity scores of NB cells and adrenal cell populations from Jansky et al. (**M**) and Kildisiute et al. (**N**) in the eight NB samples.

Figure S2. Related to Figure 2.

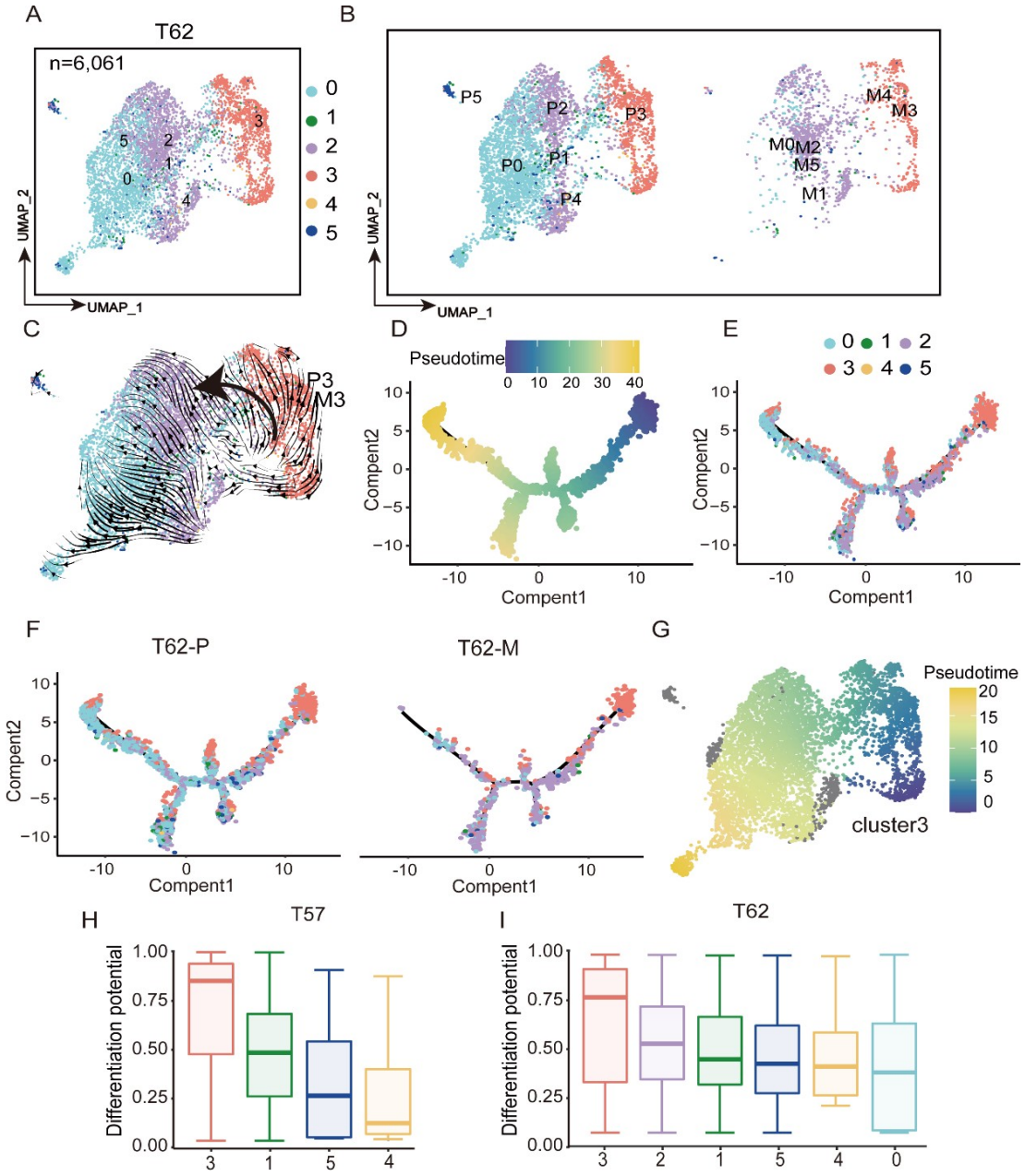

A. UMAP plots of 6,061 malignant NB cells from T62 colored by transcriptomic cluster.
B. UMAP plots split by the sample origin in T62.
C. UMAP plots showing the RNA velocity analysis of malignant NB cells in T62.
D-F. Pseudotime analysis of malignant NB cells in T62 by Monocle 2, showing the timing sequence of tumor cell progression colored by pseudotime (**D**), colored by intratumoral subpopulation (**E**), and split by the sample origin in T62 (**F**).
G. NB cell state trajectories during tumor progression inferred by Slingshot using UMAP plots according to the slingPseudotime scores in T62.
H-I. Differentiation potential of malignant NB cell populations in each cluster in T57 (**H**) and T62 (**I**) based on transcriptomic diversity. For each box, the center line indicates the median, the upper and lower boundaries indicate the 75th and 25th percentiles and the whiskers indicate the 1.5× interquartile range (IQR).

Figure S3(1 of 2). Related to Figure 3.

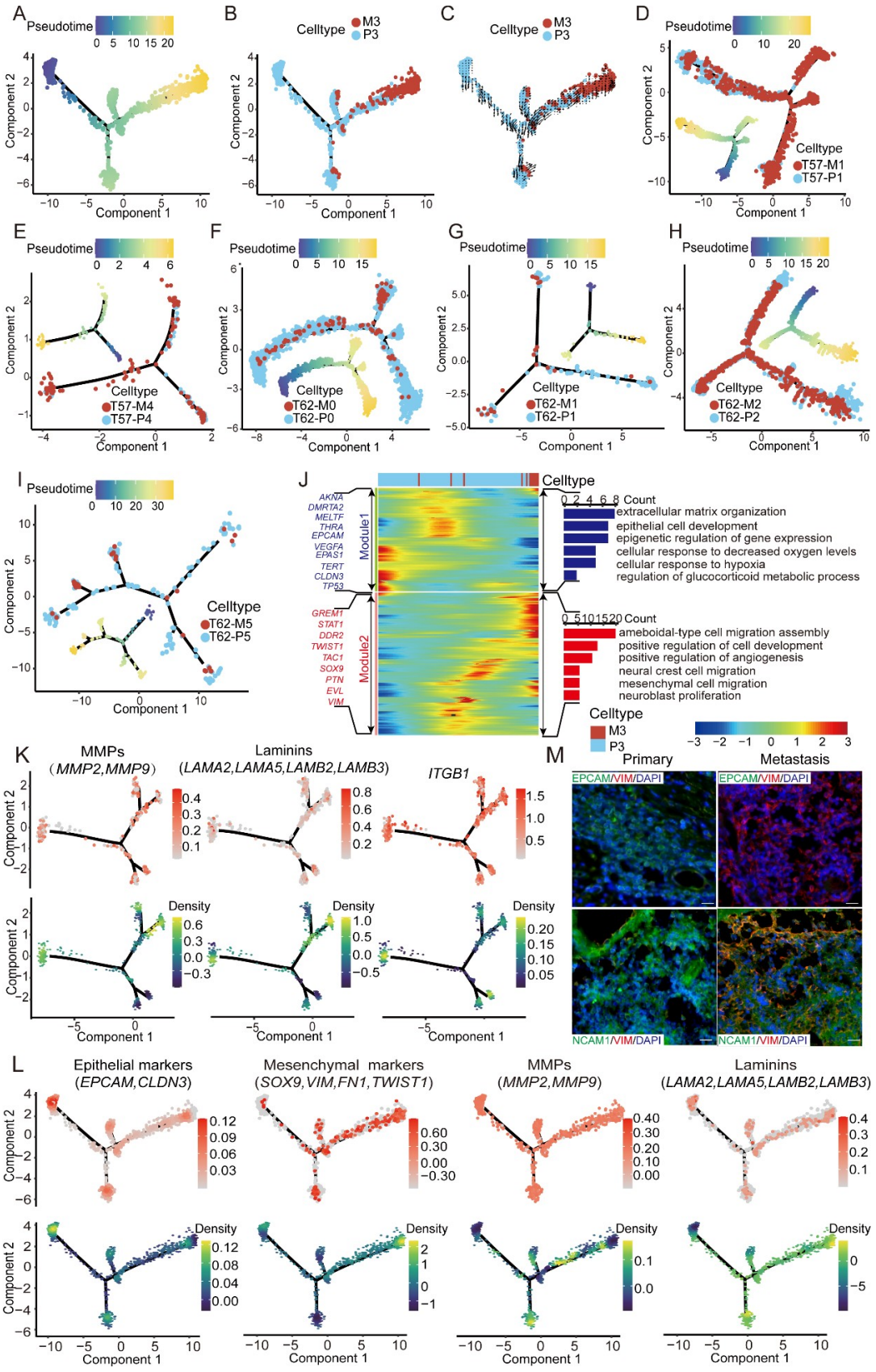

Figure S3(2 of 2). Related to Figure 3.

A-B. Pseudotime analysis of malignant NB cells from Cluster 3 in T62 by Monocle 2, showing the timing sequence of tumor cell progression colored by pseudotime (**A**) and sample origin (**B**).

C. RNA velocity analysis of malignant NB cells from Cluster 3 in the primary tumor and metastases of T62.

D. Pseudotime analysis of malignant NB cells from Cluster 1 of T57 by Monocle 2, showing the timing sequence of tumor cell progression colored by pseudotime (left) and sample origin (right).

E. Pseudotime analysis of malignant NB cells from Cluster 4 of T57 by Monocle 2, showing the timing sequence of tumor cell progression colored by pseudotime (left) and sample origin (right).

F. Pseudotime analysis of malignant NB cells from Cluster 0 of T62 by Monocle 2, showing the timing sequence of tumor cell progression colored by pseudotime (bottom) and sample origin (upper).

G. Pseudotime analysis of malignant NB cells from Cluster 1 of T62 by Monocle 2, showing the timing sequence of tumor cell progression colored by pseudotime (right) and sample origin (left).

H. Pseudotime analysis of malignant NB cells from Cluster 2 of T62 by Monocle 2, showing the timing sequence of tumor cell progression colored by pseudotime (right) and sample origin (left).

I. Pseudotime analysis of malignant NB cells from Cluster 5 of T62 by Monocle 2, showing the timing sequence of tumor cell progression colored by pseudotime (bottom) and sample origin (upper).

J. The dynamically expressed genes and enriched gene signatures were significantly associated with pseudotime from P3 to M3 in T62.

K. The expression levels (upper) and the densities (bottom) in Monocle space of MMPs (*MMP2, MMP9*), Laminins (*LAMA2, LAMA5, LAMB2, LAMB3*), and integrin β-1 (*ITGB1*) along the pseudotime trajectory from P3 to M3 in T57.

L. The expression levels (upper) and the densities (bottom) in Monocle space of epithelial markers (*EPCAM, CLDN3*), mesenchymal markers (*SOX9, VIM, FN1, TWIST1*), MMPs (*MMP2, MMP9*) and Laminins (*LAMA2, LAMA5, LAMB2, LAMB3*) along the pseudotime trajectory from P3 to M3 in T62.

M. Representative immunofluorescence staining of (primary and metastatic) human NB sections for EPCAM and VIM expression(upper), and NCAM1 and VIM expression(bottom) in patient 2. Scale bars, 20μm.

.

Figure S4(1 of 4). Related to Figure 4.

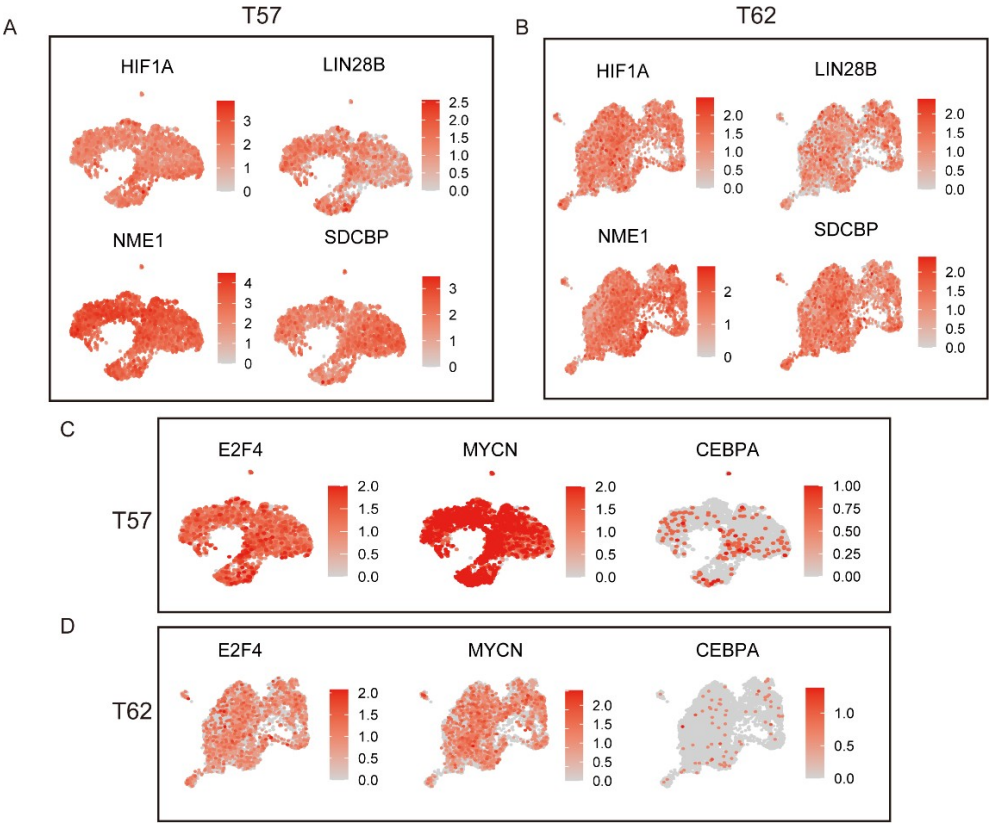

Figure S4(2 of 4). Related to Figure 4.

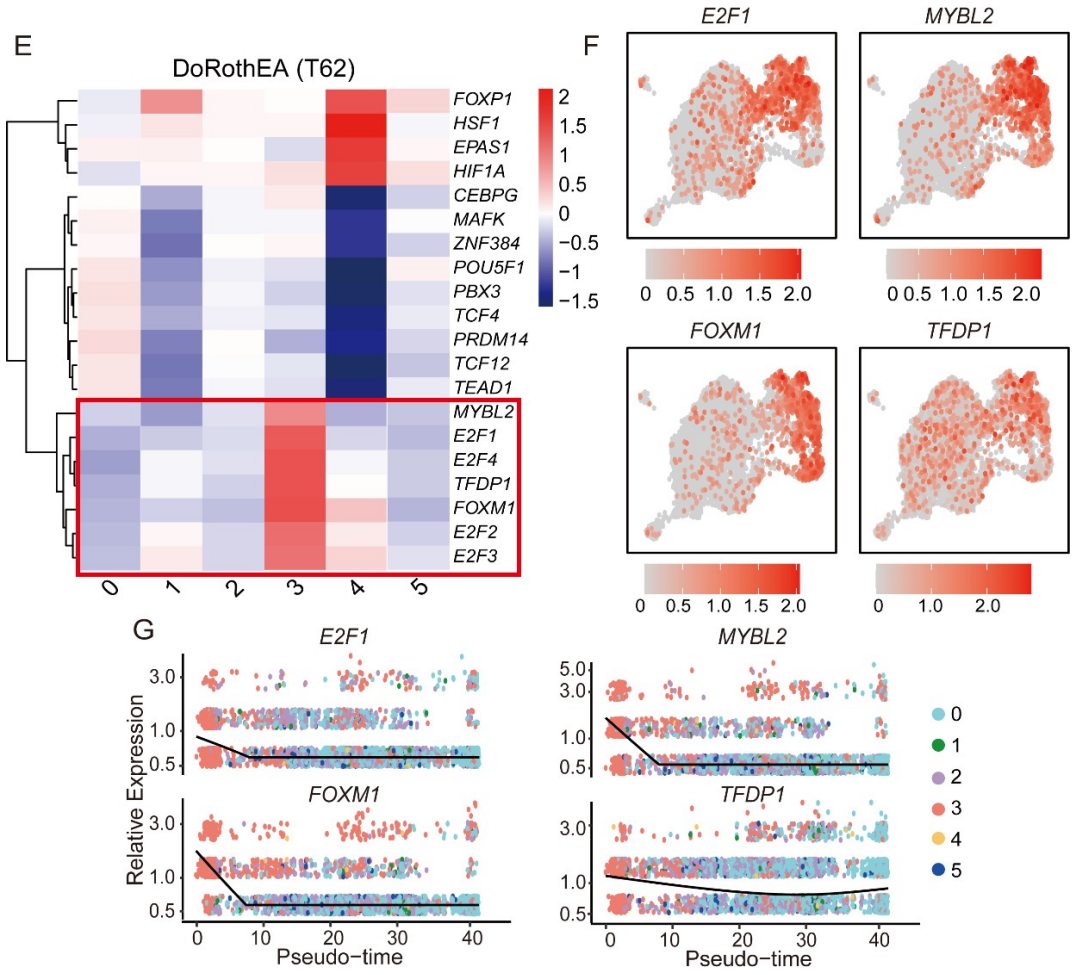

Figure S4(3 of 4). Related to Figure 4.

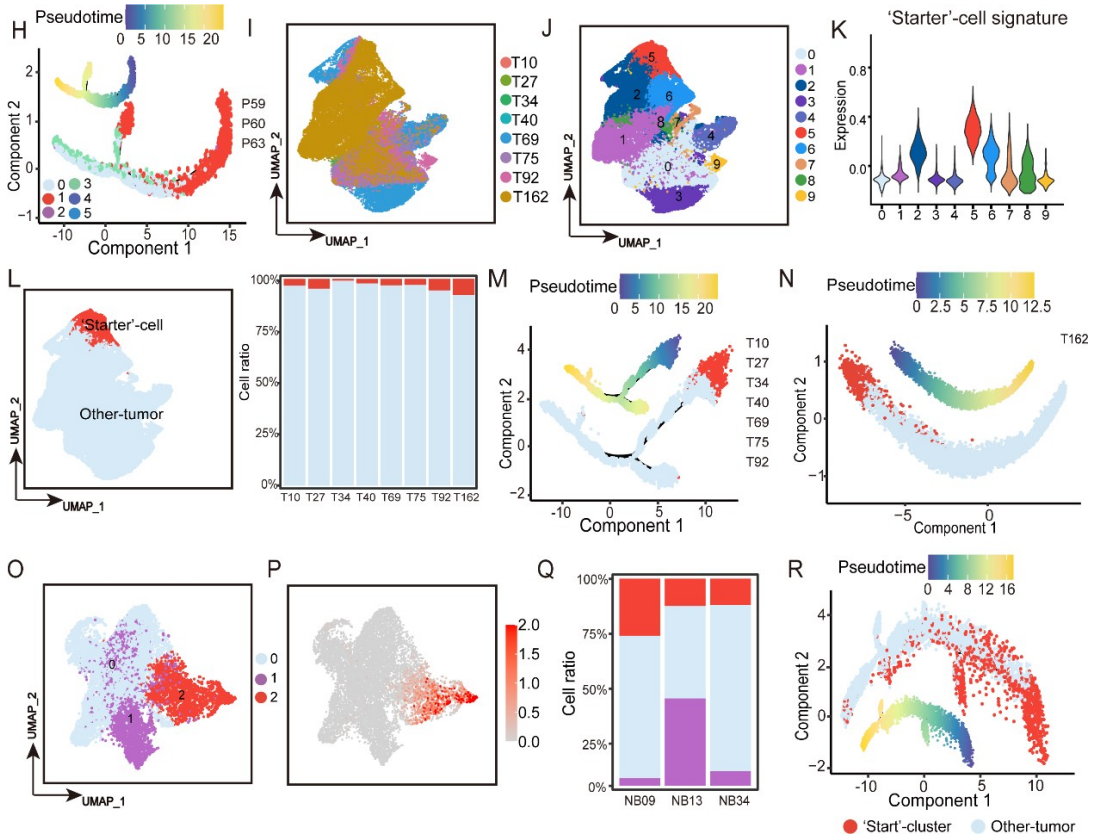

Figure S4(4 of 4). Related to Figure 4.

A-B. UMAP plots showing the expression levels and distribution of the well-known markers of NB metastasis in T57 (**A**) and T62 (**B**) (gray to red).

C-D. UMAP plots showing the expression levels and distribution of *E2F4, MYCN, and CEBPA* in T57(**C**) and T62(**D**).

E. Heatmap of the highest-scoring TFs inferred by Dorothea in each cluster in T62.

F. UMAP plots showing the expression levels and distribution of TFs in T62 based on Figure S2A (gray to red).

G. Expression of the four TFs in individual cells ordered by pseudotime along the arms of the trajectory shown in Figures S2D-E.

H. Pseudotime analysis of malignant NB cells from T59, T60, and T63 by Monocle 2, showing the timing sequence of tumor cell progression colored by pseudotime (upper) and cell clusters (bottom).

I-J. UMAP plots of the malignant NB cells from stage IV primary NB tumors with metastases in the GSE137804 dataset showing the sample origin (**I**), and transcriptomic clusters (**J**).

K. Violin plots showing the expression of the 'starter'-cell signature in different clusters.

L. UMAP plots of the malignant NB cells from the GSE137804 dataset showing the 'starter'-cell signature (left), and the proportions of this signature within each sample (right).

M-N. Pseudotime analysis of malignant NB cells in Figure S4L by Monocle 2, showing the timing sequence of tumor cell progression colored by pseudotime (upper) and the 'starter'-cell signature (bottom).

O. UMAP plots of the malignant NB cells from the relapse NB samples in the GSE147766 dataset.

P. UMAP plots showing the expression levels and distribution of the 'starter'-cell signature (gray to red).

Q. The proportions of cell clusters within each sample based on Figure S4O.

R. Pseudotime analysis of malignant NB cells in Figure S4O-P by Monocle 2, showing the timing sequence of tumor cell progression colored by pseudotime(bottom) and the 'starter'-cell signature (upper).

Figure S5 (1 of 2). Related to Figure 5.

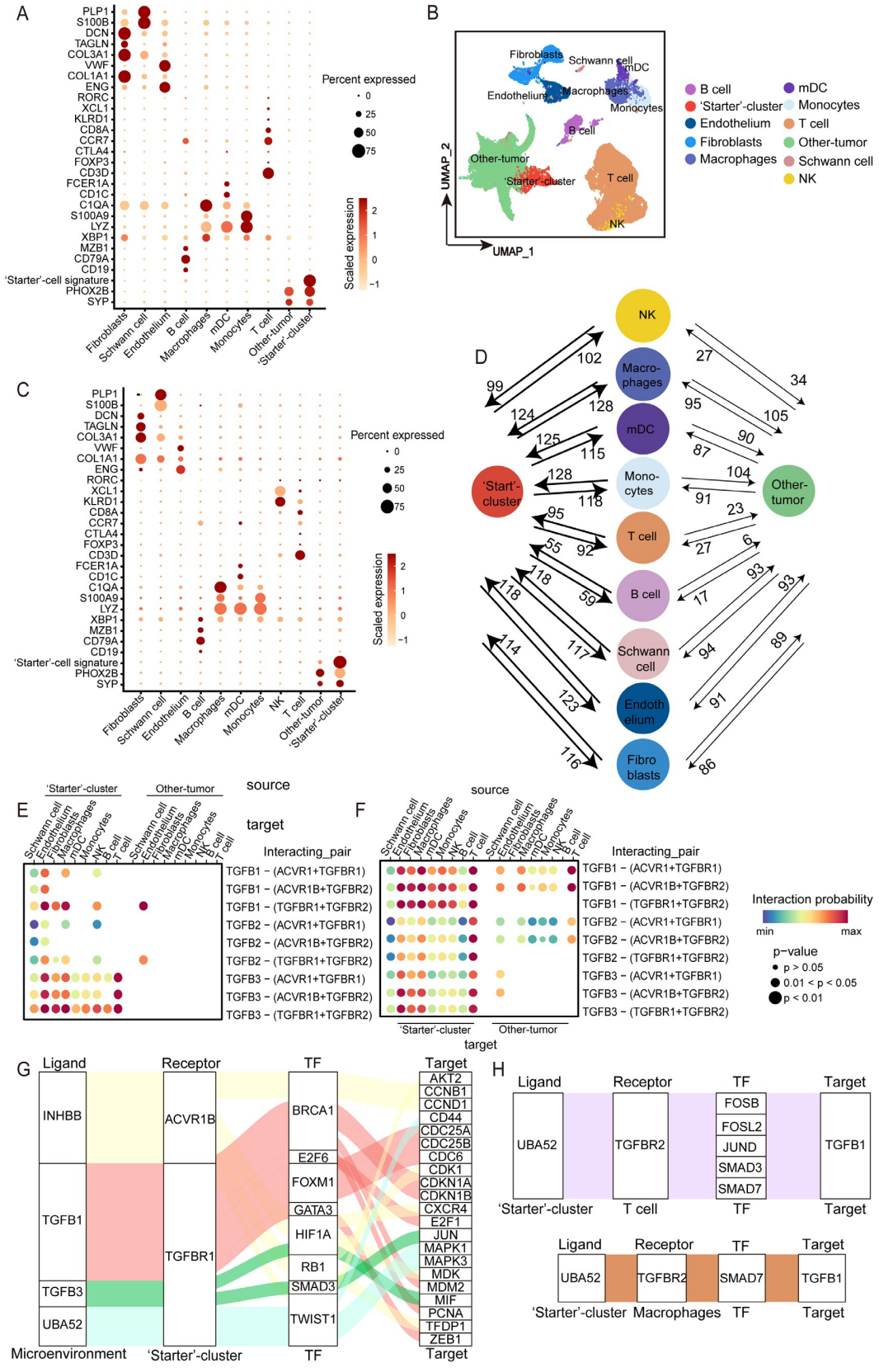

Figure S5 (2 of 2). Related to Figure 5.

A. Dot plot of signature genes of different cell types in Figure 5A.

B. UMAP plots of scRNA-seq data from the GSE147766 dataset colored by cell types.

C. Dot plot of signature genes of different cell types in Figure S5B.

D. Schematic diagram illustrating the number of receptor-ligand interactions between the microenvironment and the 'starter' cells or between the microenvironment and other tumor cells; the arrows indicate the direction of the interaction in the GSE147766 dataset

E-F. Dot plot showing the receptor-ligand pairs of the TGF-β pathway from NB cells to the microenvironment (**E**)and from the microenvironment to NB cells (**F**) in the GSE147766 dataset.

G-H. Multilayer intercellular/intracellular TGF-β signaling network between the 'starter' cells and the microenvironment both in forward (NB to microenvironment) (**G**)and in backward (microenvironment to NB) (**H**)directions in the GSE147766 dataset.

Figure S6. Related to Figure 6.

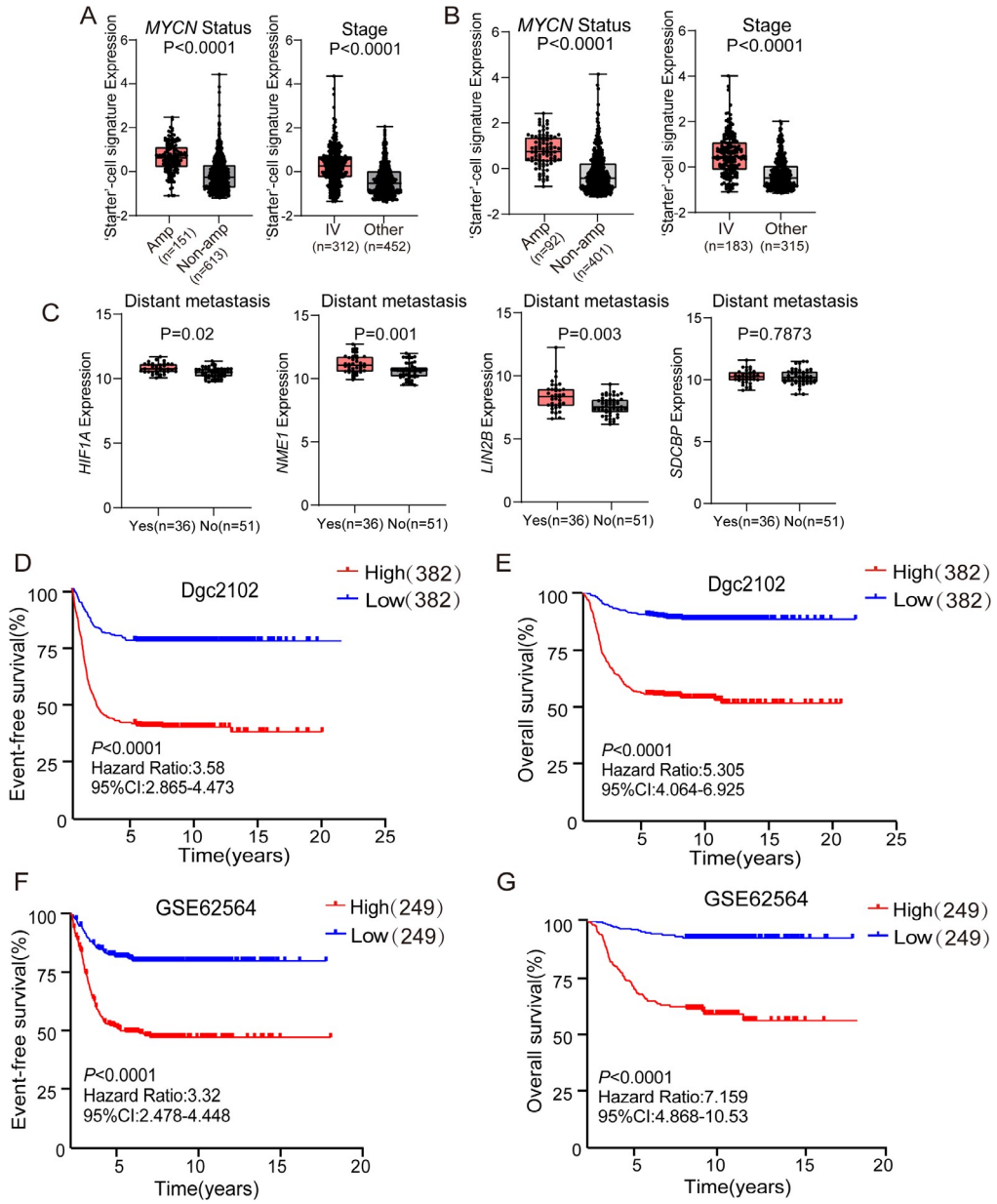

A. Boxplots of the 'starter'-cell signature expression in patients of the R2 datasets (Dgc2102), split by *MYCN* status (left, amplified versus non-amplified) or INSS staging (right, stage 4 versus stage 1, 2, 3, and 4S). The p values are reported from two-sided t-tests.

B. Boxplots of the 'starter'-cell signature expression in patients of the GSE62564 dataset, split by *MYCN* status (left, amplified versus non-amplified) or INSS staging (right, stage 4 versus stage 1, 2, 3, and 4S). The p values are reported from two-sided t-tests.

C. Boxplots showed the expression levels of *LIN28B*, *HIF1A*, *NME1*, and *SDCBP* in patients of the GSE16476 dataset, split by distant metastasis. The p values are reported from two-sided t-tests.

D-E. Kaplan–Meier plots of event-free survival (**D**) and overall survival (**E**) for 764 NB patients from the previously published R2 datasets (Dgc2102) based on the

expression levels of the ‘starter’-cell signature. Patients were divided into two groups by the median expression level of the signature (n=382 & 382 tumors in the two groups). P values were determined using the log-rank test to compare both groups.
F-**G**. Kaplan–Meier plots of event-free survival (**F**) and overall survival (**G**) for 498 NB patients from the previously published GSE62564 cohort based on the expression levels of the ‘starter’-cell signature. Patients were divided into two groups by the median expression level of the signature (n=249 & 249 tumors in the two groups). P values were determined using the log-rank test to compare both groups.

Table S1.Clinical information of the NB specimen used for single cell RNA-Seq

Tumor ID	Species	Gender	Age	WES	Histological category	INSS stage	INRG risk group	Primary tumor site	MYCN	TERT	Distant metastasis
T55	Human	Female	10Y	No	GNB(ganglioneuroblastoma)	IIA	low risk	adrenal	not amplified	—	No
T57	Human	Male	3Y4M	Yes	NB (poor differentiated)	IV	high risk	adrenal	amplified	wild type	Bone and Bone marrow
T59	Human	Female	2Y11M	Yes	NB (poor differentiated)	IV	high risk	adrenal	not amplified	wild type	Bone、Bone marrow、neck and pelvic cavity
T60	Human	Male	4Y5M	Yes	NB (poor differentiated)	IV	high risk	adrenal	not amplified	wild type	Bone marrow and lymph nodes
T62	Human	Male	6Y	Yes(primary)	NB (poor differentiated)	IV	high risk	adrenal	not amplified	wild type	Bone、Bone marrow and lymph nodes
T63	Human	Female	5Y	No	NB (poor differentiated)	IV	high risk	adrenal	not amplified	—	Bone and lymph nodes

Table S2. Basic information for single-cell datasets of eight tumor samples

Tumor ID	T55-P	T57-P	T59-P	T60-P	T62-P	T63-P	T57-M	T62-M
Estimated Number of Cells by CellRanger	2488	1322	2562	1719	5330	2085	4709	1902
Cells after QC filtering	1168	1003	2146	1425	4716	1513	2091	1385
Number of Fibroblasts	0	25	9	15	20	2	0	0
Number of immune cells	0	0	0	22	27	15	0	5
Number of malignant cells	1168	978	2137	1388	4669	1496	2091	1380

Table S3: The table shows differentially expressed genes of identified 6 cell clusters/states in NB cells

cluster	gene	p_val	avg_log2FC	pct.1	pct.2	p_val_adj
0	SLC5A7	0	1.500785312	0.781	0.118	0
0	PDE10A	0	1.379900851	0.845	0.307	0
0	ARHGAP36	0	1.355165594	0.794	0.238	0
0	DLK1	0	1.328874115	0.904	0.405	0
0	ITGA8	0	1.323036959	0.704	0.14	0
0	SLC18A2	0	1.260821824	0.893	0.555	0
0	LUZP2	0	1.218886152	0.709	0.191	0
0	PKIB	0	1.216321393	0.862	0.379	0
0	IGFBP5	0	1.197980975	0.76	0.252	0
0	AUXG01000058.1	0	1.178688257	0.973	0.653	0
0	ECEL1	0	1.158978653	0.846	0.302	0
0	PDE4D	0	0.92488025	0.611	0.184	0
0	CEP85L	0	0.914605978	0.929	0.62	0
0	CNGB1	0	0.909202106	0.841	0.504	0
0	AC007938.3	0	0.90683712	0.626	0.255	0
0	NOS1AP	0	0.897299491	0.73	0.408	0
0	EFNB2	0	0.874068535	0.813	0.515	0
0	MEST	0	0.852495354	0.984	0.709	0
0	PDE3A	0	0.842724544	0.402	0.079	0
0	PRAME	0	0.802580647	0.973	0.551	0
0	HEBP2	0	0.796135353	0.813	0.374	0
0	C11orf96	0	0.78520715	0.927	0.579	0
0	DSEL	0	0.751398178	0.833	0.541	0
0	DPP6	0	0.708260508	0.932	0.679	0
0	NDN	0	0.679659661	0.885	0.487	0
0	ARFGEF3	8.14E-302	0.834676402	0.534	0.162	1.91E-297
0	RAB3C	1.26E-283	0.780119306	0.667	0.368	2.94E-279
0	PCP4	7.64E-279	0.793005464	0.695	0.288	1.79E-274
0	CACNA2D1	1.08E-275	0.710077775	0.798	0.577	2.52E-271
0	BMP7	3.59E-272	0.655243887	0.784	0.554	8.42E-268
0	SLC2A1	3.65E-270	0.706786958	0.742	0.486	8.56E-266
0	SRGAP3	1.80E-263	0.673942462	0.859	0.624	4.21E-259
0	YPEL2	6.36E-256	0.774407678	0.647	0.345	1.49E-251
0	HAP1	5.52E-254	0.895046795	0.388	0.103	1.29E-249
0	WIPF3	1.30E-234	0.685379599	0.691	0.354	3.04E-230
0	AC005062.1	2.92E-218	0.69378105	0.555	0.233	6.84E-214

0	IGFBP2	1.04E-201	0.701599663	0.633	0.431	2.43E-197
0	ZNF208	4.99E-197	0.660881486	0.678	0.427	1.17E-192
0	NYAP2	4.13E-184	0.842153025	0.468	0.234	9.67E-180
0	SPTBN4	5.82E-157	0.706444084	0.556	0.349	1.36E-152
1	KIF5A	6.70E-130	0.367182869	0.988	0.931	1.57E-125
1	VAT1	4.63E-117	0.277164498	0.995	0.985	1.09E-112
1	KDM5B	1.23E-86	0.332042445	0.992	0.89	2.87E-82
1	KDM6B	4.41E-82	0.355758612	0.92	0.749	1.03E-77
1	SYT5	5.66E-68	0.363817721	0.838	0.626	1.33E-63
1	MIAT	1.58E-67	0.258577529	0.974	0.94	3.70E-63
1	FTX	8.10E-64	0.260068709	0.97	0.909	1.90E-59
1	LMBR1L	1.15E-59	0.316930993	0.843	0.658	2.69E-55
1	CADPS	7.52E-57	0.352567228	0.901	0.762	1.76E-52
1	ATCAY	6.51E-55	0.275963257	0.919	0.816	1.53E-50
1	SCG5	1.28E-53	0.346978259	0.801	0.584	3.01E-49
1	DDIT3	2.80E-53	0.389933378	0.869	0.72	6.56E-49
1	HIST1H2AC	2.86E-51	0.426558684	0.721	0.492	6.69E-47
1	ARMCX1	1.95E-48	0.272238557	0.915	0.803	4.57E-44
1	PNRC1	2.46E-48	0.269011352	0.959	0.838	5.75E-44
1	KDM7A	3.99E-48	0.316946771	0.786	0.59	9.35E-44
1	Z83843.1	5.84E-48	0.295460946	0.788	0.651	1.37E-43
1	NLN	2.85E-47	0.260589856	0.899	0.78	6.69E-43
1	NDRG1	1.13E-44	0.364066323	0.67	0.457	2.64E-40
1	CARD19	6.39E-44	0.268107418	0.814	0.697	1.50E-39
1	HIST2H2BE	2.09E-42	0.352511298	0.499	0.237	4.91E-38
1	C20orf194	2.33E-42	0.267585424	0.786	0.639	5.47E-38
1	MAP6	6.04E-42	0.280897727	0.797	0.608	1.42E-37
1	GABARAPL1	2.27E-41	0.310737309	0.796	0.622	5.32E-37
1	HIST3H2A	4.22E-41	0.334099324	0.687	0.419	9.89E-37
1	STX1A	9.08E-40	0.261204363	0.786	0.653	2.13E-35
1	CARS	5.03E-39	0.254562595	0.888	0.794	1.18E-34
1	MYO9A	1.15E-38	0.256146263	0.806	0.663	2.70E-34
1	HID1	1.85E-36	0.25726994	0.767	0.601	4.34E-32
1	HIST1H2BD	3.81E-34	0.317685322	0.43	0.199	8.93E-30
1	HRK	7.37E-32	0.252796572	0.924	0.875	1.73E-27
1	CARMIL2	5.15E-31	0.253141902	0.737	0.597	1.21E-26
1	NTRK3	5.08E-26	0.292452945	0.518	0.345	1.19E-21
1	SPATA2L	7.19E-26	0.250552121	0.556	0.397	1.68E-21

1	CNGB1	1.49E-20	0.263292628	0.418	0.26	3.50E-16
1	PHF24	5.08E-20	0.283852825	0.52	0.4	1.19E-15
1	USP9Y	1.68E-18	0.25780524	0.562	0.463	3.93E-14
1	CEBPB	4.97E-16	0.275283436	0.451	0.316	1.17E-11
1	ATP2B4	1.46E-15	0.291070461	0.568	0.478	3.43E-11
2	TM4SF4	0	1.254913732	0.674	0.135	0
2	TAFA4	0	1.235752137	0.684	0.117	0
2	NECAB1	0	1.173794625	0.729	0.186	0
2	SERINC5	0	0.973981195	0.685	0.282	0
2	TG	0	0.958351089	0.61	0.204	0
2	SIX3-AS1	0	0.885315655	0.506	0.132	0
2	GPM6A	0	0.867264016	0.849	0.402	0
2	FSTL5	0	0.83622054	0.42	0.075	0
2	SCD5	4.79E-303	0.84872366	0.713	0.34	1.12E-298
2	NRP2	4.20E-285	0.712617356	0.94	0.683	9.84E-281
2	HOXB-AS1	8.17E-281	0.615830031	0.336	0.05	1.91E-276
2	COX7A1	1.32E-259	0.750431288	0.52	0.159	3.09E-255
2	SPOCK1	1.56E-253	0.814659127	0.752	0.503	3.67E-249
2	SCGN	1.73E-236	0.67094704	0.331	0.062	4.06E-232
2	GPC5	1.35E-224	0.593221328	0.361	0.078	3.15E-220
2	PRCD	1.73E-217	0.739706932	0.627	0.316	4.04E-213
2	RIT2	1.85E-217	0.623521035	0.354	0.08	4.35E-213
2	PAX7	1.06E-209	0.640714239	0.392	0.102	2.49E-205
2	DDC	1.48E-204	0.628104184	0.846	0.642	3.47E-200
2	PLPPR1	1.51E-196	0.617157476	0.458	0.152	3.53E-192
2	VCAN	1.70E-193	0.686918805	0.773	0.496	3.99E-189
2	PLOD2	8.96E-193	0.555864171	0.319	0.072	2.10E-188
2	NELL1	7.46E-179	0.530884504	0.267	0.054	1.75E-174
2	TRABD2A	1.38E-177	0.631197868	0.275	0.058	3.23E-173
2	QPRT	9.54E-177	0.617031914	0.665	0.354	2.24E-172
2	SATB1-AS1	2.84E-176	0.604678557	0.376	0.121	6.66E-172
2	CGNL1	9.61E-163	0.591291134	0.425	0.145	2.25E-158
2	SEMA3E	9.19E-157	0.649087047	0.447	0.183	2.15E-152
2	EPHB6	3.62E-145	0.749837828	0.484	0.242	8.47E-141
2	LINC01833	3.66E-142	0.549902804	0.363	0.135	8.58E-138
2	CLSTN2	1.70E-140	0.634586701	0.657	0.454	3.98E-136
2	KCNIP4	2.93E-138	0.572267256	0.558	0.288	6.88E-134
2	ITPR2	4.06E-138	0.584662657	0.436	0.186	9.52E-134

2	CRH	6.91E-138	1.020212345	0.519	0.26	1.62E-133
2	RPRM	3.85E-131	0.644285854	0.469	0.244	9.01E-127
2	OSBPL10	3.47E-130	0.534556157	0.675	0.432	8.14E-126
2	PRKCB	2.71E-125	0.599479192	0.576	0.336	6.36E-121
2	DUSP23	3.63E-119	0.577430271	0.588	0.379	8.49E-115
2	ERICH3	5.33E-119	0.547797888	0.493	0.253	1.25E-114
2	SEMA6A	9.79E-115	0.567782386	0.531	0.324	2.29E-110
3	MKI67	0	1.866424388	0.938	0.099	0
3	TOP2A	0	1.823134838	0.981	0.29	0
3	TPX2	0	1.693156542	0.942	0.226	0
3	UBE2C	0	1.668274531	0.882	0.156	0
3	CENPF	0	1.663751978	0.957	0.321	0
3	NUSAP1	0	1.65190403	0.888	0.117	0
3	BIRC5	0	1.628305684	0.909	0.163	0
3	NUF2	0	1.591362929	0.898	0.145	0
3	RRM2	0	1.587366124	0.831	0.066	0
3	ASPM	0	1.585903211	0.809	0.085	0
3	KIFC1	0	1.525602321	0.869	0.092	0
3	CKAP2L	0	1.484389525	0.832	0.065	0
3	GTSE1	0	1.475139731	0.867	0.128	0
3	NDC80	0	1.456558445	0.832	0.079	0
3	CCNA2	0	1.443121869	0.809	0.07	0
3	FOXM1	0	1.431944626	0.873	0.116	0
3	NCAPG	0	1.411224316	0.857	0.123	0
3	KNL1	0	1.406683201	0.842	0.138	0
3	PTTG1	0	1.39617124	0.796	0.174	0
3	CDK1	0	1.372831683	0.806	0.088	0
3	AURKB	0	1.36572513	0.731	0.032	0
3	SPC25	0	1.353980239	0.761	0.052	0
3	MAD2L1	0	1.345923927	0.895	0.277	0
3	SMC4	0	1.345211168	0.983	0.504	0
3	TACC3	0	1.334602783	0.789	0.091	0
3	PRC1	0	1.322810932	0.983	0.477	0
3	HIST1H3B	0	1.317546177	0.654	0.055	0
3	CDKN3	0	1.28876372	0.713	0.092	0
3	CDCA8	0	1.283594808	0.667	0.055	0
3	KIF23	0	1.28007821	0.7	0.039	0
3	PRR11	0	1.276907284	0.771	0.133	0

3	MYBL2	0	1.272314646	0.797	0.168	0
3	CDCA5	0	1.270253405	0.812	0.132	0
3	KIF2C	0	1.26330757	0.746	0.056	0
3	ENDOG	0	1.25733949	0.918	0.405	0
3	NCAPH	0	1.254426582	0.819	0.133	0
3	TYMS	0	1.252705887	0.898	0.402	0
3	KIF4A	0	1.252483933	0.72	0.053	0
3	ARHGAP11A	0	1.233279146	0.74	0.105	0
3	PBK	0	1.227513656	0.745	0.071	0
4	HSPA6	0	2.488759499	0.955	0.021	0
4	BAG3	0	1.654760814	0.829	0.059	0
4	SERPINH1	5.50E-208	1.342002292	0.573	0.052	1.29E-203
4	DNAJA4	1.00E-152	1.55117929	0.874	0.212	2.34E-148
4	RRAD	1.87E-133	0.816487643	0.447	0.048	4.38E-129
4	POU3F2	2.87E-124	0.853447633	0.608	0.098	6.72E-120
4	HBEGF	5.87E-117	0.94690227	0.653	0.124	1.37E-112
4	HSPA1B	6.03E-113	1.612127174	0.92	0.35	1.41E-108
4	IER5	7.87E-104	1.369342384	0.844	0.277	1.84E-99
4	AL627171.2	5.80E-97	1.227504746	0.93	0.403	1.36E-92
4	MTRNR2L8	1.60E-95	1.038880829	0.799	0.241	3.74E-91
4	DGKE	1.55E-94	1.064276556	0.884	0.337	3.63E-90
4	HSPB1	4.83E-90	1.28141865	0.99	0.717	1.13E-85
4	ZFAND2A	1.47E-88	1.17675788	0.985	0.605	3.44E-84
4	C1orf52	1.06E-86	0.957284474	0.95	0.503	2.48E-82
4	LINC00324	5.49E-86	0.882033324	0.553	0.116	1.29E-81
4	TSPYL2	1.84E-78	0.992854746	0.854	0.335	4.32E-74
4	TENT5A	2.99E-77	0.971576498	0.789	0.259	7.01E-73
4	ABHD3	2.28E-75	0.855344403	0.724	0.217	5.34E-71
4	PCDH9	3.52E-74	0.921451002	0.779	0.257	8.25E-70
4	USPL1	1.13E-73	1.056502405	0.879	0.414	2.66E-69
4	DNAJB4	3.12E-72	0.911522681	0.709	0.223	7.31E-68
4	JMJD6	4.07E-72	0.886075327	0.94	0.566	9.53E-68
4	RGS2	2.91E-71	0.927500634	0.874	0.358	6.83E-67
4	LINC00632	4.40E-71	0.939073047	0.839	0.298	1.03E-66
4	TENT4B	1.13E-70	0.929529464	0.874	0.42	2.66E-66
4	NEFM	6.52E-69	0.960324851	0.864	0.352	1.53E-64
4	ZNF503	6.59E-68	0.935493407	0.879	0.403	1.54E-63
4	SNHG17	9.03E-66	0.877436156	0.879	0.426	2.12E-61

4	MT-ATP8	3.03E-65	0.945029371	0.899	0.503	7.11E-61
4	SIRT7	4.85E-65	0.818460037	0.894	0.445	1.14E-60
4	ATG101	9.91E-65	0.819068412	0.91	0.497	2.32E-60
4	GADD45G	3.43E-64	0.928247187	0.814	0.341	8.03E-60
4	SNHG15	8.40E-63	0.861882782	0.92	0.53	1.97E-58
4	SPTY2D1	2.09E-62	0.84225704	0.92	0.501	4.89E-58
4	MEG3	4.23E-58	0.998192472	0.894	0.347	9.91E-54
4	SNHG5	9.79E-57	0.834342576	0.925	0.574	2.29E-52
4	ARRDC3	3.84E-54	0.895566849	0.889	0.492	9.01E-50
4	AC108134.2	8.18E-52	0.906758516	0.372	0.082	1.92E-47
5	COL11A1	3.45E-147	0.694901292	0.215	0.008	8.09E-143
5	PSMB8	1.82E-127	0.611052145	0.251	0.014	4.27E-123
5	HLA-B	5.12E-99	0.799738769	0.215	0.013	1.20E-94
5	MT1E	1.02E-79	0.707362625	0.23	0.02	2.39E-75
5	GALR1	2.57E-70	0.756174045	0.23	0.023	6.03E-66
5	HLA-C	1.42E-63	1.112176223	0.361	0.064	3.34E-59
5	HLA-A	2.27E-62	1.173437371	0.414	0.084	5.32E-58
5	LXN	5.88E-49	0.812535634	0.304	0.055	1.38E-44
5	TMEFF2	1.38E-45	0.707658243	0.272	0.049	3.23E-41
5	IRF1	2.72E-28	0.87777501	0.377	0.13	6.38E-24
5	MT2A	2.84E-28	1.063489842	0.393	0.142	6.64E-24
5	DMD	1.15E-25	0.662087833	0.366	0.127	2.69E-21
5	MT1X	1.85E-24	0.775888631	0.346	0.12	4.34E-20
5	DLG2	1.53E-21	0.688219178	0.319	0.117	3.58E-17
5	NDN	5.52E-21	0.538793922	0.827	0.593	1.29E-16
5	PCP4	7.57E-21	0.724798429	0.681	0.396	1.77E-16
5	AL391807.1	1.74E-18	0.690500036	0.607	0.374	4.07E-14
5	MT1F	2.20E-17	0.688440928	0.387	0.178	5.15E-13
5	JUNB	6.07E-16	0.724171659	0.56	0.36	1.42E-11
5	HEBP2	3.65E-15	0.547209846	0.723	0.492	8.56E-11
5	MX2	8.39E-14	0.42675547	0.398	0.191	1.97E-09

Table S4. Enriched upregulated pathways in the cells of Cluster 3 versus other malignant cells

ID	Description	setSize	enrichmentScore	NES	pvalue
GO:0007059	chromosome segregation	277	0.743397739	3.151944	1.00E-10
GO:0000819	sister chromatid segregation	169	0.772257657	3.150741	1.00E-10
GO:0098813	nuclear chromosome segregation	218	0.746397292	3.119725	1.00E-10
GO:0006261	DNA-dependent DNA replication	133	0.79423063	3.118339	1.00E-10
GO:0000070	mitotic sister chromatid segregation	146	0.780811618	3.111837	1.00E-10
GO:0006260	DNA replication	223	0.740643776	3.094712	1.00E-10
GO:0000280	nuclear division	314	0.710312962	3.044647	1.00E-10
GO:0140014	mitotic nuclear division	231	0.715878838	3.001781	1.00E-10
GO:0048285	organelle fission	348	0.686364635	2.967359	1.00E-10
GO:0051321	meiotic cell cycle	157	0.732574274	2.962042	1.00E-10
GO:0000075	cell cycle checkpoint signaling	141	0.73898075	2.934647	1.00E-10
GO:0000725	recombinational repair	117	0.756801038	2.934147	1.00E-10
GO:0051983	regulation of chromosome segregation	75	0.797763314	2.920215	1.00E-10
GO:1903046	meiotic cell cycle process	123	0.747816997	2.917613	1.00E-10
GO:0000724	double-strand break repair via homologous recombination	116	0.753492593	2.915946	1.00E-10
GO:0007093	mitotic cell cycle checkpoint signaling	108	0.7555324	2.891991	1.00E-10
GO:0140013	meiotic nuclear division	110	0.748422228	2.877401	1.00E-10
GO:1901988	negative regulation of cell cycle phase transition	175	0.697848085	2.866998	1.00E-10
GO:0051304	chromosome separation	78	0.773599701	2.846859	1.00E-10
GO:0010948	negative regulation of cell cycle process	205	0.679508167	2.82129	1.00E-10
GO:0061982	meiosis I cell cycle process	81	0.763475155	2.821176	1.00E-10
GO:0033045	regulation of sister chromatid segregation	62	0.798995484	2.819279	1.00E-10
GO:0006310	DNA recombination	216	0.676878853	2.817893	1.00E-10
GO:0006281	DNA repair	429	0.641805664	2.816797	1.00E-10
GO:0006302	double-strand break repair	212	0.676841636	2.815648	1.00E-10
GO:0051301	cell division	472	0.632944535	2.793827	1.00E-10
GO:0007127	meiosis I	77	0.762223312	2.793817	1.00E-10
GO:0010965	regulation of mitotic sister chromatid separation	57	0.809998033	2.79267	1.00E-10
GO:0044786	cell cycle DNA replication	36	0.878273622	2.785233	1.00E-10
GO:1905818	regulation of chromosome separation	61	0.792546323	2.781206	1.00E-10
GO:0051306	mitotic sister chromatid separation	58	0.803716528	2.77785	1.00E-10
GO:0071103	DNA conformation change	171	0.678191482	2.763809	1.00E-10
GO:0090068	positive regulation of cell cycle process	150	0.689007399	2.760453	1.00E-10
GO:1901987	regulation of cell cycle phase transition	268	0.653375342	2.758166	1.00E-10
GO:0007088	regulation of mitotic nuclear division	83	0.743261239	2.756492	1.00E-10
GO:1901990	regulation of mitotic cell cycle phase transition	209	0.66277179	2.756135	1.00E-10
GO:0007091	metaphase/anaphase transition of mitotic cell cycle	56	0.802219002	2.754647	1.00E-10
GO:1901991	negative regulation of mitotic cell cycle phase transition	125	0.705802254	2.748935	1.00E-10

GO:0044784	metaphase/anaphase transition of cell cycle	57	0.797130433	2.748305	1.00E-10
GO:0031570	DNA integrity checkpoint signaling	103	0.723145448	2.744873	1.00E-10
GO:0010564	regulation of cell cycle process	450	0.621773451	2.73839	1.00E-10
GO:0030071	regulation of mitotic metaphase/anaphase transition	54	0.796848152	2.715771	1.00E-10
GO:1902749	regulation of cell cycle G2/M phase transition	78	0.7367265	2.711165	1.00E-10
GO:0032508	DNA duplex unwinding	72	0.743642583	2.705281	1.00E-10
GO:1902099	regulation of metaphase/anaphase transition of cell cycle	55	0.791594844	2.704382	1.00E-10
GO:0051783	regulation of nuclear division	95	0.715154319	2.701175	1.00E-10
GO:0044770	cell cycle phase transition	366	0.623024315	2.700693	1.00E-10
GO:0033260	nuclear DNA replication	32	0.87932211	2.696448	1.00E-10
GO:0010389	regulation of G2/M transition of mitotic cell cycle	73	0.739331145	2.692377	1.00E-10
GO:0044839	cell cycle G2/M phase transition	111	0.697502305	2.685138	1.00E-10
GO:0045930	negative regulation of mitotic cell cycle	162	0.659662873	2.684673	1.00E-10
GO:0044772	mitotic cell cycle phase transition	306	0.627668718	2.68282	1.00E-10
GO:0090329	regulation of DNA-dependent DNA replication	40	0.832013304	2.6822	1.00E-10
GO:0045132	meiotic chromosome segregation	58	0.775407325	2.680006	1.00E-10
GO:0032392	DNA geometric change	78	0.725165066	2.668619	1.00E-10
GO:0000086	G2/M transition of mitotic cell cycle	104	0.700750564	2.663187	1.00E-10
GO:0007346	regulation of mitotic cell cycle	314	0.61653701	2.642691	1.00E-10
GO:0044774	mitotic DNA integrity checkpoint signaling	71	0.726804315	2.636126	1.00E-10
GO:0007051	spindle organization	163	0.647101788	2.631886	1.00E-10
GO:0045786	negative regulation of cell cycle	256	0.623586658	2.630875	1.00E-10
GO:0000077	DNA damage checkpoint signaling	95	0.696358468	2.630182	1.00E-10
GO:0045787	positive regulation of cell cycle	202	0.628604962	2.6146	1.00E-10
GO:0033046	negative regulation of sister chromatid segregation	38	0.822229939	2.613384	1.00E-10
GO:0033048	negative regulation of mitotic sister chromatid segregation	38	0.822229939	2.613384	1.00E-10
GO:2000816	negative regulation of mitotic sister chromatid separation	38	0.822229939	2.613384	1.00E-10
GO:0033047	regulation of mitotic sister chromatid segregation	41	0.802143691	2.610663	1.00E-10
GO:0051985	negative regulation of chromosome segregation	39	0.814949345	2.604216	1.00E-10
GO:1905819	negative regulation of chromosome separation	39	0.814949345	2.604216	1.00E-10
GO:0006275	regulation of DNA replication	85	0.700722826	2.601333	1.00E-10
GO:0044773	mitotic DNA damage checkpoint signaling	67	0.723299602	2.595291	1.00E-10
GO:0070192	chromosome organization involved in meiotic cell cycle	40	0.804570975	2.593733	1.00E-10
GO:0045841	negative regulation of mitotic metaphase/anaphase transition	37	0.814863268	2.583074	1.00E-10
GO:0007098	centrosome cycle	112	0.669339677	2.579869	1.00E-10
GO:0045839	negative regulation of mitotic nuclear division	44	0.783357782	2.571558	1.00E-10
GO:1902850	microtubule cytoskeleton organization involved in mitosis	128	0.655523246	2.567094	1.00E-10
GO:0007094	mitotic spindle assembly checkpoint signaling	35	0.814613515	2.566044	1.00E-10
GO:0071173	spindle assembly checkpoint signaling	35	0.814613515	2.566044	1.00E-10
GO:0071174	mitotic spindle checkpoint signaling	35	0.814613515	2.566044	1.00E-10

GO:1902100	negative regulation of metaphase/anaphase transition of cell cycle	38	0.807167099	2.565509	1.00E-10
GO:2001251	negative regulation of chromosome organization	76	0.697055274	2.558672	1.00E-10
GO:0031577	spindle checkpoint signaling	36	0.80650871	2.557648	1.74E-10
GO:0045005	DNA-dependent DNA replication maintenance of fidelity	42	0.785277462	2.551418	1.00E-10
GO:0006323	DNA packaging	93	0.674823528	2.54776	1.00E-10
GO:0051784	negative regulation of nuclear division	49	0.754670712	2.537589	1.00E-10
GO:0007131	reciprocal meiotic recombination	40	0.782577391	2.522831	2.94E-10
GO:0140527	reciprocal homologous recombination	40	0.782577391	2.522831	2.94E-10
GO:0007052	mitotic spindle organization	109	0.654681446	2.51789	1.00E-10
GO:0034508	centromere complex assembly	28	0.853715718	2.51695	1.00E-10
GO:0008608	attachment of spindle microtubules to kinetochore	32	0.818741204	2.510676	3.89E-10
GO:0006270	DNA replication initiation	31	0.82649046	2.510611	1.41E-10
GO:0035825	homologous recombination	42	0.771315758	2.506055	3.93E-10
GO:0031023	microtubule organizing center organization	120	0.64392545	2.505317	1.00E-10
GO:0051310	metaphase plate congression	60	0.7150297	2.503894	3.15E-10
GO:0033044	regulation of chromosome organization	162	0.614750918	2.501892	1.00E-10
GO:0030261	chromosome condensation	27	0.848290725	2.487639	1.84E-10
GO:0042770	signal transduction in response to DNA damage	137	0.627868256	2.486488	1.00E-10
GO:0034502	protein localization to chromosome	79	0.674753473	2.485698	1.00E-10
GO:0022616	DNA strand elongation	21	0.888510115	2.475533	1.59E-10
GO:0051383	kinetochore organization	22	0.88057926	2.46808	1.33E-10
GO:0051303	establishment of chromosome localization	70	0.681249979	2.459403	5.62E-10
GO:0036297	interstrand cross-link repair	34	0.790055708	2.458754	3.40E-09
GO:0065004	protein-DNA complex assembly	104	0.64385825	2.446969	1.00E-10
GO:0050000	chromosome localization	72	0.672348567	2.445922	9.93E-10
GO:1901989	positive regulation of cell cycle phase transition	80	0.659867122	2.437868	4.11E-10
GO:0051225	spindle assembly	101	0.64040863	2.426267	1.00E-10
GO:0031297	replication fork processing	36	0.762895225	2.419338	2.69E-08
GO:0051302	regulation of cell division	101	0.636860963	2.412827	1.02E-10
GO:0032465	regulation of cytokinesis	69	0.669689817	2.409473	5.72E-09
GO:1901992	positive regulation of mitotic cell cycle phase transition	65	0.679879174	2.407746	4.09E-09
GO:0006284	base-excision repair	40	0.746094315	2.405219	2.47E-08
GO:0010972	negative regulation of G2/M transition of mitotic cell cycle	46	0.72226577	2.399189	1.72E-08
GO:0007062	sister chromatid cohesion	49	0.712137308	2.39457	1.71E-08
GO:1902750	negative regulation of cell cycle G2/M phase transition	47	0.719526841	2.39394	1.82E-08
GO:0044818	mitotic G2/M transition checkpoint	38	0.752179008	2.390734	1.04E-08
GO:0007080	mitotic metaphase plate congression	47	0.717199991	2.386198	2.34E-08
GO:0071459	protein localization to chromosome, centromeric region	24	0.826382532	2.380216	3.28E-08
GO:0071897	DNA biosynthetic process	128	0.605243531	2.370194	1.00E-10
GO:0007099	centriole replication	36	0.743573697	2.358065	1.47E-07

GO:0140694	non-membrane-bounded organelle assembly	273	0.553970962	2.34763	1.00E-10
GO:0051298	centrosome duplication	62	0.663364095	2.3407	2.89E-08
GO:0098534	centriole assembly	37	0.734918285	2.329653	5.64E-08
GO:0009262	deoxyribonucleotide metabolic process	33	0.75027749	2.329071	3.78E-07
GO:0045143	homologous chromosome segregation	34	0.747906086	2.327579	2.60E-07
GO:1902969	mitotic DNA replication	13	0.92401821	2.325285	7.04E-09
GO:0034501	protein localization to kinetochore	18	0.860633655	2.323153	4.88E-08
GO:1903083	protein localization to condensed chromosome	18	0.860633655	2.323153	4.88E-08
GO:0006271	DNA strand elongation involved in DNA replication	15	0.919801276	2.320183	1.81E-10
GO:0071824	protein-DNA complex subunit organization	135	0.58588747	2.312953	2.98E-10
GO:0000226	microtubule cytoskeleton organization	449	0.522548227	2.300984	1.00E-10
GO:0007095	mitotic G2 DNA damage checkpoint signaling	29	0.770824464	2.300679	6.70E-07
GO:0045931	positive regulation of mitotic cell cycle	86	0.615747951	2.291994	1.42E-08
GO:0010212	response to ionizing radiation	110	0.593949257	2.283511	3.20E-09
GO:0000727	double-strand break repair via break-induced replication	11	0.937976301	2.25458	1.34E-08
GO:0006312	mitotic recombination	21	0.802719128	2.236506	2.76E-06
GO:1902751	positive regulation of cell cycle G2/M phase transition	27	0.761710091	2.233738	1.22E-06
GO:0000076	DNA replication checkpoint signaling	15	0.882614053	2.226379	4.90E-08
GO:0051382	kinetochore assembly	17	0.83016122	2.217626	2.69E-06
GO:0009411	response to UV	114	0.573435536	2.213822	1.62E-08
GO:0090307	mitotic spindle assembly	57	0.639723162	2.205605	6.03E-07
GO:0016572	histone phosphorylation	31	0.725811739	2.204781	6.49E-06
GO:0019692	deoxyribose phosphate metabolic process	30	0.730453599	2.203939	2.52E-06
GO:2000779	regulation of double-strand break repair	74	0.600836715	2.197539	9.49E-07
GO:0006298	mismatch repair	25	0.758533594	2.193992	6.19E-06
GO:0000731	DNA synthesis involved in DNA repair	24	0.760670316	2.190946	9.75E-06
GO:0007143	female meiotic nuclear division	22	0.780776136	2.188353	5.08E-06
GO:0000018	regulation of DNA recombination	70	0.605662508	2.186522	1.44E-06
GO:1901976	regulation of cell cycle checkpoint	29	0.731539274	2.183425	1.13E-05
GO:0006282	regulation of DNA repair	107	0.569754631	2.180449	1.32E-07
GO:0010569	regulation of double-strand break repair via homologous recombination	42	0.670740313	2.179279	4.25E-06
GO:2000104	negative regulation of DNA-dependent DNA replication	13	0.864648956	2.175883	6.52E-06
GO:1901657	glycosyl compound metabolic process	52	0.639457533	2.175232	3.90E-06
GO:0010971	positive regulation of G2/M transition of mitotic cell cycle	24	0.753817941	2.171209	1.33E-05
GO:0006220	pyrimidine nucleotide metabolic process	38	0.681555814	2.166264	3.70E-06
GO:0045740	positive regulation of DNA replication	33	0.69636486	2.161711	2.19E-05
GO:0072527	pyrimidine-containing compound metabolic process	53	0.634974198	2.157335	3.35E-06
GO:0034724	DNA replication-independent nucleosome organization	16	0.824692012	2.148361	6.17E-06
GO:0009394	2'-deoxyribonucleotide metabolic process	29	0.719751371	2.148241	2.45E-05
GO:0007076	mitotic chromosome condensation	15	0.851330514	2.147467	1.43E-06

GO:0006301	postreplication repair	25	0.739621133	2.13929	2.05E-05
GO:0051315	attachment of mitotic spindle microtubules to kinetochore	15	0.846378773	2.134976	2.02E-06
GO:0051307	meiotic chromosome separation	17	0.793512269	2.119725	2.89E-05
GO:0007292	female gamete generation	71	0.583036073	2.114677	4.39E-06
GO:0051785	positive regulation of nuclear division	25	0.72798548	2.105634	4.13E-05
GO:0000910	cytokinesis	135	0.532660438	2.102825	2.01E-07
GO:0051445	regulation of meiotic cell cycle	27	0.716783982	2.101991	3.75E-05
GO:0000082	G1/S transition of mitotic cell cycle	139	0.530990531	2.101127	3.42E-07
GO:0009116	nucleoside metabolic process	35	0.666945306	2.100887	5.70E-05
GO:0006336	DNA replication-independent nucleosome assembly	15	0.832191828	2.09919	6.97E-06
GO:0009123	nucleoside monophosphate metabolic process	52	0.616397903	2.096791	1.44E-05
GO:0008156	negative regulation of DNA replication	23	0.733672428	2.095602	3.77E-05
GO:0006287	base-excision repair, gap-filling	12	0.854335036	2.095212	1.63E-05
GO:0000079	regulation of cyclin-dependent protein serine/threonine kinase activity	71	0.577023225	2.092868	6.13E-06
GO:0051984	positive regulation of chromosome segregation	13	0.831197547	2.091702	4.63E-05
GO:0000212	meiotic spindle organization	12	0.851031156	2.08711	2.04E-05
GO:0044843	cell cycle G1/S phase transition	152	0.520975876	2.08602	3.23E-07
GO:0009314	response to radiation	291	0.489040751	2.084272	1.01E-10
GO:0051054	positive regulation of DNA metabolic process	148	0.521834806	2.084068	1.94E-07
GO:0071478	cellular response to radiation	124	0.533417451	2.080829	3.76E-07
GO:0009147	pyrimidine nucleoside triphosphate metabolic process	19	0.763922832	2.07899	2.88E-05
GO:0000723	telomere maintenance	114	0.537883167	2.076568	8.07E-07
GO:0090231	regulation of spindle checkpoint	14	0.828273991	2.07525	3.60E-05
GO:0090266	regulation of mitotic cell cycle spindle assembly checkpoint	14	0.828273991	2.07525	3.60E-05
GO:1903504	regulation of mitotic spindle checkpoint	14	0.828273991	2.07525	3.60E-05
GO:0032200	telomere organization	115	0.536668661	2.073226	1.07E-06
GO:0051988	regulation of attachment of spindle microtubules to kinetochore	13	0.823158149	2.071471	7.30E-05
GO:0032467	positive regulation of cytokinesis	26	0.708983407	2.0653	8.01E-05
GO:0000722	telomere maintenance via recombination	12	0.842048103	2.065079	3.85E-05
GO:0051781	positive regulation of cell division	40	0.640376712	2.064412	7.50E-05
GO:0031571	mitotic G1 DNA damage checkpoint signaling	25	0.713579714	2.063967	9.11E-05
GO:0044819	mitotic G1/S transition checkpoint signaling	25	0.713579714	2.063967	9.11E-05
GO:0051052	regulation of DNA metabolic process	257	0.488388944	2.061059	1.06E-09
GO:0007140	male meiotic nuclear division	24	0.714657369	2.058416	0.000101
GO:0006268	DNA unwinding involved in DNA replication	15	0.815867162	2.058011	2.41E-05
GO:0045739	positive regulation of DNA repair	57	0.596763272	2.05749	1.63E-05
GO:2000045	regulation of G1/S transition of mitotic cell cycle	82	0.553767145	2.052087	8.54E-06
GO:0046599	regulation of centriole replication	18	0.759533236	2.050248	9.81E-05
GO:2001020	regulation of response to DNA damage stimulus	172	0.502257072	2.049718	1.51E-07
GO:0007129	homologous chromosome pairing at meiosis	26	0.702869646	2.04749	0.000115

GO:0006977	DNA damage response, signal transduction by p53 class mediator resulting in cell cycle arrest	15	0.80947572	2.041889	3.63E-05
GO:1904029	regulation of cyclin-dependent protein kinase activity	74	0.558076566	2.041145	2.08E-05
GO:0009263	deoxyribonucleotide biosynthetic process	12	0.827845972	2.030249	9.76E-05
GO:0031497	chromatin assembly	61	0.578367259	2.029608	4.17E-05
GO:0006760	folic acid-containing compound metabolic process	21	0.728204579	2.028896	0.000142
GO:0009124	nucleoside monophosphate biosynthetic process	33	0.653163307	2.027602	0.000252
GO:0031100	animal organ regeneration	41	0.622952609	2.027466	6.05E-05
GO:0009219	pyrimidine deoxyribonucleotide metabolic process	18	0.750859495	2.026834	0.000138
GO:0006333	chromatin assembly or disassembly	81	0.548272275	2.025963	1.97E-05
GO:0034644	cellular response to UV	70	0.560199063	2.022393	2.89E-05
GO:0045840	positive regulation of mitotic nuclear division	21	0.720937221	2.008648	0.000186
GO:2000781	positive regulation of double-strand break repair	33	0.646999756	2.008468	0.000347
GO:0042558	pteridine-containing compound metabolic process	27	0.683976431	2.005782	0.000224
GO:0051653	spindle localization	39	0.627028778	2.003705	0.000176
GO:0009200	deoxyribonucleoside triphosphate metabolic process	14	0.798575162	2.00084	0.000159
GO:0001833	inner cell mass cell proliferation	12	0.815834498	2.000792	0.000185
GO:0019985	translesion synthesis	16	0.767897499	2.000409	0.000157
GO:0009264	deoxyribonucleotide catabolic process	21	0.715967629	1.994802	0.000223
GO:0046386	deoxyribose phosphate catabolic process	21	0.715967629	1.994802	0.000223
GO:0040001	establishment of mitotic spindle localization	26	0.684104582	1.992827	0.000283
GO:0072331	signal transduction by p53 class mediator	120	0.511091368	1.9885	7.93E-06
GO:0006334	nucleosome assembly	45	0.601378805	1.982738	0.000232
GO:0072528	pyrimidine-containing compound biosynthetic process	25	0.685248843	1.982022	0.000379
GO:0051293	establishment of spindle localization	35	0.62871411	1.980459	0.000386
GO:0010165	response to X-ray	25	0.682246003	1.973337	0.000438
GO:0006978	DNA damage response, signal transduction by p53 class mediator resulting in transcription of p21 class mediator	13	0.78366859	1.972096	0.00053
GO:0000281	mitotic cytokinesis	62	0.558502781	1.970694	0.000154
GO:2000134	negative regulation of G1/S transition of mitotic cell cycle	48	0.587534103	1.96732	0.000242
GO:0031573	mitotic intra-S DNA damage checkpoint signaling	14	0.783615506	1.963358	0.000335
GO:0046546	development of primary male sexual characteristics	71	0.541205329	1.962957	6.65E-05
GO:0008584	male gonad development	70	0.542621545	1.958936	0.000104
GO:2000105	positive regulation of DNA-dependent DNA replication	12	0.797720286	1.956367	0.00048
GO:0022412	cellular process involved in reproduction in multicellular organism	181	0.47450575	1.955963	1.60E-06
GO:0072711	cellular response to hydroxyurea	10	0.831700053	1.951357	0.000361
GO:2001022	positive regulation of response to DNA damage stimulus	78	0.529983188	1.950347	6.54E-05
GO:1902806	regulation of cell cycle G1/S phase transition	94	0.515727904	1.94935	4.27E-05
GO:0072710	response to hydroxyurea	11	0.810409256	1.947951	0.000705
GO:0001832	blastocyst growth	17	0.728956609	1.947276	0.000671
GO:0071482	cellular response to light stimulus	80	0.526169788	1.943925	0.000112
GO:1902807	negative regulation of cell cycle G1/S phase transition	50	0.577034841	1.943317	0.000331

GO:0001556	oocyte maturation	17	0.727291043	1.942827	0.000731
GO:0001325	formation of extrachromosomal circular DNA	13	0.769031377	1.935262	0.000973
GO:0090656	t-circle formation	13	0.769031377	1.935262	0.000973
GO:0090737	telomere maintenance via telomere trimming	13	0.769031377	1.935262	0.000973
GO:0043486	histone exchange	16	0.742865344	1.935199	0.000528
GO:0046605	regulation of centrosome cycle	41	0.593269567	1.930859	0.000267
GO:0048477	oogenesis	48	0.575829671	1.928129	0.000427
GO:0006221	pyrimidine nucleotide biosynthetic process	22	0.687800914	1.927762	0.001084
GO:0007064	mitotic sister chromatid cohesion	24	0.666251055	1.918992	0.000923
GO:2000573	positive regulation of DNA biosynthetic process	52	0.563216205	1.915883	0.000491
GO:0042772	DNA damage response, signal transduction resulting in transcription	14	0.76422541	1.914776	0.000768
GO:0030330	DNA damage response, signal transduction by p53 class mediator	53	0.562950896	1.912635	0.000324
GO:0051782	negative regulation of cell division	11	0.79559879	1.912352	0.001353
GO:0007096	regulation of exit from mitosis	12	0.779595706	1.911918	0.000997
GO:0009148	pyrimidine nucleoside triphosphate biosynthetic process	14	0.762902141	1.91146	0.000815
GO:0006730	one-carbon metabolic process	21	0.685680984	1.910418	0.000647
GO:0000729	DNA double-strand break processing	16	0.732569735	1.908378	0.000863
GO:0007063	regulation of sister chromatid cohesion	20	0.694208869	1.907953	0.001097
GO:0061640	cytoskeleton-dependent cytokinesis	83	0.513404308	1.904035	0.00013
GO:0000712	resolution of meiotic recombination intermediates	13	0.755423356	1.901017	0.001736
GO:0016446	somatic hypermutation of immunoglobulin genes	11	0.789669928	1.898101	0.001563
GO:0009112	nucleobase metabolic process	23	0.662826928	1.893245	0.001089
GO:1904666	regulation of ubiquitin protein ligase activity	19	0.695358017	1.892393	0.000914
GO:2000241	regulation of reproductive process	62	0.536122777	1.891725	0.000483
GO:0071479	cellular response to ionizing radiation	52	0.555337287	1.889082	0.000634
GO:0002566	somatic diversification of immune receptors via somatic mutation	12	0.767475204	1.882193	0.001546
GO:0010639	negative regulation of organelle organization	267	0.444506761	1.878083	5.12E-07
GO:0046661	male sex differentiation	81	0.507811881	1.876455	0.0002
GO:0010457	centriole-centriole cohesion	13	0.742901767	1.869507	0.002769
GO:0010824	regulation of centrosome duplication	37	0.589678564	1.86925	0.000568
GO:0034728	nucleosome organization	74	0.510324931	1.866495	0.000427
GO:0009162	deoxyribonucleoside monophosphate metabolic process	14	0.744063184	1.864259	0.001894
GO:0048599	oocyte development	24	0.646935819	1.863359	0.001766
GO:0042398	cellular modified amino acid biosynthetic process	34	0.597241008	1.85869	0.001286
GO:0060045	positive regulation of cardiac muscle cell proliferation	10	0.791268178	1.856494	0.001626
GO:0097421	liver regeneration	22	0.662367821	1.856479	0.00245
GO:0090305	nucleic acid phosphodiester bond hydrolysis	190	0.448453336	1.855149	1.40E-05
GO:0009994	oocyte differentiation	25	0.641378007	1.85513	0.002214
GO:1901293	nucleoside phosphate biosynthetic process	163	0.45585878	1.854064	2.52E-05
GO:0006289	nucleotide-excision repair	54	0.542594237	1.849238	0.000552

GO:1990748	cellular detoxification	54	0.54251958	1.848983	0.000559
GO:0051299	centrosome separation	13	0.734498028	1.848359	0.003678
GO:0046653	tetrahydrofolate metabolic process	15	0.731818308	1.845999	0.001412
GO:2000042	negative regulation of double-strand break repair via homologous recombination	16	0.708167645	1.84481	0.002257
GO:0090399	replicative senescence	10	0.786141813	1.844467	0.001914
GO:0007100	mitotic centrosome separation	12	0.751046135	1.841902	0.002729
GO:0072332	intrinsic apoptotic signaling pathway by p53 class mediator	53	0.541181079	1.838672	0.000854
GO:0045910	negative regulation of DNA recombination	28	0.622652341	1.835722	0.002281
GO:0035563	positive regulation of chromatin binding	10	0.782194088	1.835205	0.002049
GO:0070601	centromeric sister chromatid cohesion	10	0.778998948	1.827708	0.002422
GO:0048469	cell maturation	76	0.497270332	1.825324	0.000519
GO:0098869	cellular oxidant detoxification	47	0.547925512	1.823004	0.001606
GO:0006206	pyrimidine nucleobase metabolic process	12	0.741622589	1.818791	0.004281
GO:0006081	cellular aldehyde metabolic process	31	0.596749789	1.812733	0.00295
GO:0007141	male meiosis I	15	0.717231587	1.809205	0.002268
GO:0009636	response to toxic substance	127	0.461590251	1.80793	0.000126
GO:0051294	establishment of spindle orientation	24	0.627523172	1.807445	0.00337
GO:0031099	regeneration	99	0.476504564	1.806908	0.000374
GO:0006266	DNA ligation	16	0.692605953	1.804271	0.003858
GO:0046112	nucleobase biosynthetic process	16	0.691092044	1.800327	0.004043
GO:0032069	regulation of nuclease activity	17	0.673811716	1.799967	0.005028
GO:0097237	cellular response to toxic substance	60	0.513715586	1.798931	0.001548
GO:0006739	NADP metabolic process	25	0.621360575	1.797231	0.004689
GO:0009141	nucleoside triphosphate metabolic process	78	0.487746285	1.794914	0.000729
GO:0008630	intrinsic apoptotic signaling pathway in response to DNA damage	68	0.495416116	1.783593	0.001058
GO:0051642	centrosome localization	25	0.614779148	1.778195	0.005585
GO:0061842	microtubule organizing center localization	26	0.610154302	1.777406	0.004741
GO:0000132	establishment of mitotic spindle orientation	21	0.63744323	1.77602	0.004052
GO:0001824	blastocyst development	74	0.48513238	1.774354	0.0017
GO:0071398	cellular response to fatty acid	22	0.632631213	1.773133	0.006497
GO:0009060	aerobic respiration	146	0.444849801	1.772899	0.000141
GO:0009165	nucleotide biosynthetic process	162	0.434837504	1.769686	0.000138
GO:0098754	detoxification	61	0.503402371	1.766541	0.002247
GO:0045842	positive regulation of mitotic metaphase/anaphase transition	14	0.703946453	1.763746	0.005917
GO:1901970	positive regulation of mitotic sister chromatid separation	14	0.703946453	1.763746	0.005917
GO:1902101	positive regulation of metaphase/anaphase transition of cell cycle	14	0.703946453	1.763746	0.005917
GO:0009416	response to light stimulus	199	0.423589662	1.759901	0.000116
GO:0071168	protein localization to chromatin	23	0.616065834	1.75968	0.005759
GO:0071214	cellular response to abiotic stimulus	195	0.423564675	1.758016	0.000107
GO:0104004	cellular response to environmental stimulus	195	0.423564675	1.758016	0.000107

GO:0031145	anaphase-promoting complex-dependent catabolic process	18	0.650236776	1.755218	0.00472
GO:0007569	cell aging	82	0.472913272	1.752468	0.001248
GO:0009223	pyrimidine deoxyribonucleotide catabolic process	14	0.69911937	1.751652	0.006364
GO:0006244	pyrimidine nucleotide catabolic process	16	0.669723415	1.744661	0.007382
GO:0030262	apoptotic nuclear changes	16	0.668686246	1.741959	0.00763
GO:0009410	response to xenobiotic stimulus	226	0.416388135	1.740803	5.69E-05
GO:0002200	somatic diversification of immune receptors	51	0.511424104	1.734888	0.003604
GO:0006575	cellular modified amino acid metabolic process	103	0.45682858	1.734003	0.001566
GO:0009129	pyrimidine nucleoside monophosphate metabolic process	14	0.691611137	1.73284	0.007649
GO:0010332	response to gamma radiation	41	0.532180576	1.732039	0.004202
GO:1905820	positive regulation of chromosome separation	15	0.680996119	1.717801	0.00647
GO:0008406	gonad development	111	0.446131876	1.71745	0.00105
GO:0006303	double-strand break repair via nonhomologous end joining	58	0.49626699	1.715226	0.004655
GO:0055086	nucleobase-containing small molecule metabolic process	346	0.395940511	1.710411	3.54E-06
GO:0042773	ATP synthesis coupled electron transport	70	0.472952999	1.707423	0.00484
GO:0042775	mitochondrial ATP synthesis coupled electron transport	70	0.472952999	1.707423	0.00484
GO:2000278	regulation of DNA biosynthetic process	78	0.46355563	1.705892	0.002286
GO:0006753	nucleoside phosphate metabolic process	301	0.39900061	1.704326	1.42E-05
GO:0007281	germ cell development	133	0.432964598	1.699922	0.000588
GO:0071466	cellular response to xenobiotic stimulus	72	0.466804443	1.698178	0.002594
GO:0006304	DNA modification	75	0.460889437	1.687087	0.003369
GO:0045137	development of primary sexual characteristics	115	0.435631574	1.682906	0.002026
GO:0009142	nucleoside triphosphate biosynthetic process	61	0.477773588	1.676605	0.005324
GO:0006766	vitamin metabolic process	55	0.489076675	1.670867	0.006781
GO:2001021	negative regulation of response to DNA damage stimulus	63	0.473267569	1.670779	0.004866
GO:0043648	dicarboxylic acid metabolic process	59	0.479459299	1.66898	0.006332
GO:0006119	oxidative phosphorylation	104	0.437507551	1.662738	0.001949
GO:0022904	respiratory electron transport chain	84	0.446813001	1.654839	0.004523
GO:0009117	nucleotide metabolic process	298	0.387259257	1.654269	5.24E-05
GO:0007276	gamete generation	339	0.383647383	1.653145	4.52E-05
GO:0045333	cellular respiration	174	0.402310946	1.649549	0.000996
GO:0031109	microtubule polymerization or depolymerization	100	0.430074594	1.630945	0.005808
GO:0072593	reactive oxygen species metabolic process	108	0.418325798	1.601247	0.003403
GO:0034614	cellular response to reactive oxygen species	89	0.426520585	1.595371	0.007624
GO:0007548	sex differentiation	135	0.402431403	1.58871	0.003789
GO:0022900	electron transport chain	119	0.406357749	1.580941	0.003749
GO:0051656	establishment of organelle localization	288	0.370343136	1.574771	0.00028
GO:0051053	negative regulation of DNA metabolic process	86	0.422628711	1.573148	0.007406
GO:0048232	male gamete generation	264	0.371698764	1.568745	0.00026
GO:0048609	multicellular organismal reproductive process	396	0.358143061	1.560116	0.000174

GO:0032504	multicellular organism reproduction	399	0.356579351	1.555448	0.000162
GO:0019953	sexual reproduction	403	0.351258786	1.533253	0.000281
GO:0044282	small molecule catabolic process	208	0.366986537	1.526493	0.004337
GO:0007568	aging	193	0.366903122	1.522643	0.004183
GO:0032886	regulation of microtubule-based process	180	0.368480264	1.51801	0.006437
GO:0000302	response to reactive oxygen species	128	0.38721351	1.516367	0.007299
GO:0006325	chromatin organization	259	0.353805968	1.492658	0.001958
GO:1901615	organic hydroxy compound metabolic process	256	0.349569911	1.474815	0.003981
GO:0008284	positive regulation of cell population proliferation	412	0.337186338	1.472197	0.000702
GO:0007283	spermatogenesis	255	0.34606294	1.459697	0.005786
GO:0051347	positive regulation of transferase activity	310	0.338768293	1.450505	0.0027
GO:0044703	multi-organism reproductive process	485	0.324803322	1.434047	0.0017
GO:0044283	small molecule biosynthetic process	297	0.325976141	1.390868	0.007926
GO:0003006	developmental process involved in reproduction	457	0.313524968	1.381424	0.004939
GO:0051129	negative regulation of cellular component organization	470	0.30476577	1.344911	0.006319

Table S5.The 'starter'-cell signature for Cluster 3. Top 150 genes identified by Seurat function FindAllMarkers.

TOP2A	ECT2	TROAP	KIF2C	CKS1B
MKI67	CCNB1	SKA3	DHFR	HMMR
CENPF	HIST1H1B	DBF4	NCAPH	DTYMK
BIRC5	ORC6	HIST1H4C	FBXO5	NCAPD2
UBE2C	PCNA	H2AFX	TK1	MND1
TPX2	UBE2T	NEK2	CDKN3	GMNN
NUSAP1	MCM10	MCM3	KIF11	MXD3
NUF2	HIST1H1C	CIT	KIF4A	FEN1
RRM2	RACGAP1	SYNE2	C21orf58	FAM111B
ASPM	CENPW	WDR34	CENPU	PHF19
GTSE1	BUB1B	ZNF367	KIF23	RFC3
FOXM1	CKAP2	GINS2	SGO1	CDC45
SMC4	KIF15	BRIP1	DIAPH3	E2F1
KIFC1	ESCO2	HIST1H2AG	ANP32E	CDT1
TYMS	BRCA1	TRIM59	ARHGAP11A	CIP2A
NDC80	PKMYT1	WDR76	CDCA8	CDC20
CKAP2L	DTL	DEPDC1	HIST1H3D	KIF20B
PRC1	CCNB2	RRM1	RAD51AP1	SMC2
MAD2L1	SKA1	PARPBP	CENPE	LMNB1
PTTG1	XRCC2	ANLN	KIF20A	
NCAPG	ZWINT	ASF1B		
CCNA2	DLGAP5	CDC6		
CDK1	BRCA2	BLM		
MYBL2	KIF22	PIMREG		
ENDOG	MIS18BP1	MASTL		
KNL1	SGO2	HELLS		
SPC25	CKS2	PLK1		
HIST1H3B	NCAPG2	CENPN		
HMGB2	MELK	E2F2		
PCLAF	CENPK	INCENP		
ATAD2	CEP152	KIF18B		
PRR11	CENPH	FANCD2		
CLSPN	HJURP	CENPM		
PBK	KIF14	DSN1		
TACC3	TTK	HIST1H1E		
AURKB	SPAG5	ATAD5		
CDCA5	FANCI	EXO1		

Table S6. Reagents, accession numbers and software

REAGENT or RESOURCE	SOURCE	IDENTIFIER
Antibodies or Chemicals		
DAPI Solution	BD Biosciences	Cat# 564907
PE Anti-Human CD45	Biolegend	Cat# 304008; RRID:AB_314396
DMEM medium	Gibco	Cat# C11995500BT
DMEM/F-12	Gibco	Cat# C11330500BT
Fetal Bovine Serum	Biological Industries	Cat# 04-001-1ACS
MEM NEAA(100×)	Gibco	Cat# 11140-050
Penicillin-Streptomycin-Glutamine (100X) Gibco™	Gibco	Cat# 15140-122
MACS Tissue Storage Solution	Miltenyi Biotec	Cat# 130-100-008
DNase I	Sigma-Aldrich	Cat# D4527
Red Blood Cell Lysis Buffer	Solarbio	Cat# R1010
Phosphate Buffered Saline	Biological Industries	Cat# 02-024-1ACS
Anti -NCAM1 Rabbit mAb	Abcam	Cat# ab220360; RRID:AB_2927664
Anti -EPCAM Rabbit mAb	Cell Signaling Technology	Cat# 14452s; RRID:AB_2736866
Anti -VIM Mouse mAb	Sigma	Cat# V5255; RRID:AB_477625
Goat anti-Rabbit IgG (H+L) Cross-Adsorbed Secondary Antibody, Alexa Fluor 488	Thermo Fisher Scientific	Cat# A-11008; RRID: AB_143165
Goat anti-Mouse IgG (H+L) Cross-Adsorbed Secondary Antibody, Alexa Fluor	Thermo Fisher Scientific	Cat# A-21422; RRID: AB_141822
Critical Commercial Assays		
Tumor Cell Isolation Kit, human	Miltenyi Biotec	Cat# 130-108-339
Chromium Single Cell 3' Library & Gel Bead Kit	10x Genomics	PN-120267
Deposited Data		
ScRNA-seq of Human NB	This paper	GSE223374
Human neuroblastoma scRNA-seq data (Dong et al., 2020)	GEO	GSE137804
Human neuroblastoma scRNA-seq data (Verhoeven et al., 2022)	GEO	GSE147766
Human neuroblastoma microarray data (Su et al., 2014)	GEO	GSE62564
Human neuroblastoma microarray data (dgc2102,2020)	R2	http://r2.amc.nl
Human neuroblastoma microarray data	GEO	GSE16476
Human neuroblastoma microarray data (E-MTAB-8248,2019)	R2	http://r2.amc.nl
ScRNA-seq of Human fetal adrenal glands (Jansky, S et al., 2021)	European Genome-phenome Archive	EGAS00001004388
ScRNA-seq of Human fetal adrenal glands (Kildisiute, G et al., 2021)	/	http://neuroblastomacellatlas.org
Software and Algorithms		
GraphPad Prism 8	GraphPad Software Inc.	http://www.graphpad.com
FlowJo	FlowJo Software	https://www.flowjo.com/
Gene Set Enrichment Analysis (GSEA)	Broad Institute	http://software.broadinstitute.org/gsea
Cell Ranger (v.4.0.0)	Cell Ranger Single Cell Software	https://support.10xgenomics.com/single-
Seurat(v.4.0.0)	Seurat R package	https://satijalab.org/seurat/
ClusterProfiler(v3.18.1)	ClusterProfiler R package	https://bioconductor.org/packages/clust
FastQC (v.0.11.8)	FastQC Software	http://www.bioinformatics.babraham.ac.u
Human genome GRCh38	N/A	ftp://ftp.ensembl.org/pub/release-94/
DESeq2 (v.1.20.0)	Love et al.2014	https://bioconductor.org/packages/DESeq

R (v.4.0.0)	The R Project for Statistical	http://www.r-project.org
Monocle2	Trapnell et al.2014	http://www.bioconductor.org/packages/release/bioc/html/monocle.html
velocyto	La Manno et al.2018	https://velocyto.org/
scVelo (v.0.1.20)	Bergen et al., 2020	https://scvelo-notebooks.readthedocs.io/index.html
Slingshot (v.2.4.0)	Street K et al. 2018	https://bioconductor.org/packages/release/bioc/vignettes/slingshot/inst/doc/vi
InferCNV	GitHub	https://github.com/broadinstitute/inferCNV
DoRothEA (v.1.9.0)	Garcia-Alonso L et al.2019	https://saezlab.github.io/DoRothEA/.
SingleR(v.1.0.5)	GitHub	https://github.com/dviraran/SingleR
Harmony (v.1.0)	Korsunsky I et al.2019	https://github.com/immunogenomics/harmony
CytoTRACE (v.0.3.3)	Gulati GS et al.2020	https://cytotrace.stanford.edu/
Python (v. 3.8.6)	Python Software Foundation	https://www.python.org/
scikit-learn(v. 0.24.2)	N/A	scikit-learn: machine learning in Python - scikit-learn 0.24.2 documentation
bcftools (v. 1.8)	GitHub	https://github.com/samtools/bcftools
DoubletFinder(v.2.0.3)	McGinnis CS et al.2019	https://github.com/chris-mcginnis-ucsf/DoubletFinder
BWA (v.0.7.17)	Li H et al. 2009	Maq (sourceforge.net)
scMLnet	Zhang J et al. 2020	https://github.com/SunXQlab/scMLnet